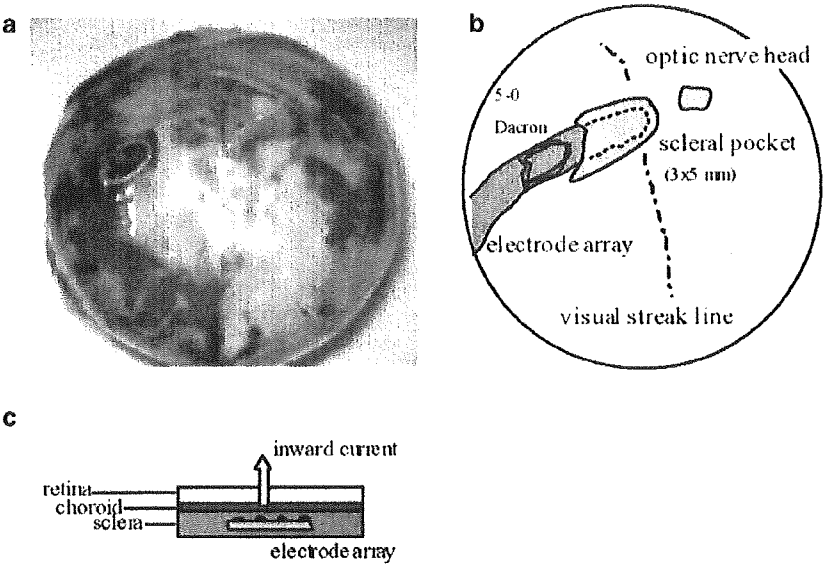

Fig. 2 **a** A photograph of an enucleated rabbit eye which has the microelectrode array implanted into the scleral pocket. **b** A schematic diagram of the electrode array that is inserted into a 3×5-mm scleral pocket over the visual streak. **c** A schematic diagram of transretinal electrical stimulation

Recording electrode

After exposing the skull, a stainless steel recording electrode was screwed into the skull bone above the visual cortex. The position of the electrode was 8 mm rostral to the lambda suture and 7 mm lateral to the midline [1, 8]. The reference needle stainless steel electrode was then placed between the skin and skull near the ear.

To confirm that the recording electrode was placed over the visual cortex, visual evoked potentials (VEPs) elicited by photic stimuli (1.2 J, 15 cm from the cornea) were recorded. The EEPs were elicited by monophasic electrical pulses of 0.5 ms duration, and 50 responses were averaged. A bandpass filter of 5 Hz to 1 kHz was used.

Electrical threshold current

The electric current was changed from 10 μA to 700 μA, and the direction of the current was first set for inward-flowing currents (electrode array positive and reference electrode negative), then the polarity was reversed for outward-flowing currents (electrode array negative and reference electrode positive).

For the purpose of finding the threshold current, the amplitudes of the EEPs elicited by a current of 500 μA delivered by each of the eight electrodes were compared. The electrode which elicited the largest EEP was selected to determine the threshold current. With this electrode, the electric current was decreased in steps, and the minimum electric current that elicited the first or second positive peak of the EEP (P_1 or P_2) was defined as the threshold current. The threshold current was also determined by reversing the polarity of the stimulating current.

Histology

At the completion of the experiment, the rabbit was killed by an overdose of barbiturate (100 mg/kg), and the eye was enucleated for histological examination. The eyes were embedded in paraffin, and 10-μm sections were cut and stained with hematoxylin and eosin (HE staining). Light microscopy was used to evaluate tissue damage. The electrode array used for stimulation was examined after the experiment with a scanning electron microscope.

Results

The electrode arrays were inserted and positioned without complications, and the placement of the recording electrode into the rabbit's skull was also completed without complications. Although the overall experiment time was only 3–4 h, early adverse effects were not detected in the eyes and brains surrounding the stimulating and recording electrodes.

The VEPs consisted of three large positive waves (Fig. 3a). The mean implicit time of the first positive peak (P_{v1}) was 23.8±1.2 ms, the second peak (P_{v2}) was 41.0± 3.0 ms, and the third peak (P_{v3}) was 58.2±2.1 ms (mean± SEM; n=6).

EEPs were also recorded in all rabbits. The mean implicit times of the EEP with an inward current (amplitude 500 μA; duration 0.5 ms) were 15.7±2.0 ms for P_{i1}, 27.3± 0.6 ms for P_{i2}, and 41.2±0.9 ms for P_{i3} (Fig. 3b). The implicit time of P_{i1} was significantly shorter than that for P_{v1}.

The waveform of EEPs with outward current with the same stimulus parameters consisted of four peaks, which were slightly different from that evoked by inward currents. The implicit times were 19.3±0.7 ms for P_{o1}, 30.1±

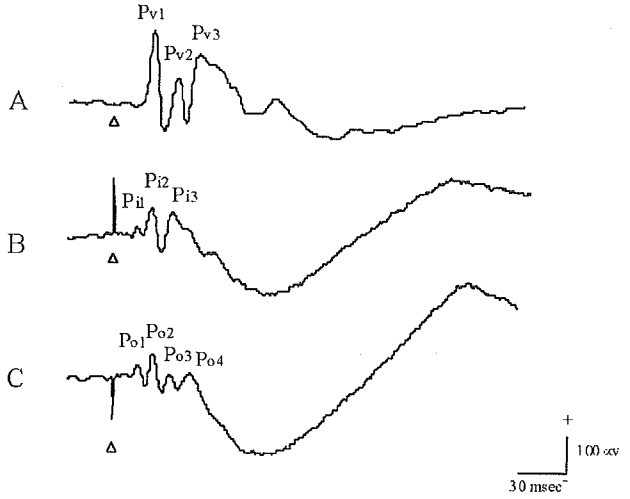

Fig. 3 Typical waveforms of VEP and EEPs. **a** VEP consists of three large positive components. The first positive peak (P_{v1}) had an implicit time of 24 ms, the second positive peak (P_{v2}) had an implicit time of 41 ms, and the third positive peak (P_{v3}) had an implicit time of 58 ms. **b** EEP with inward current (sclera+/vitreous−) shows an upward artifact at the onset of the stimulation. The first positive peak (P_{i1}) had an implicit time of 16 ms, a second positive peak (P_{i2}) had an implicit time of 27 ms, and a third positive peak (P_{i3}) had an implicit time of 41 ms. **c** EEP with outward current (sclera−/vitreous +) shows a negative downward artifact at the time of stimulation. The first positive peak (P_{o1}) had an implicit time of 19 ms, the second positive peak (P_{o2}) had an implicit time of 30 ms, a third positive peak (P_{o3}) had an implicit time of 42 ms, and a fourth positive peak (P_{o4}) had an implicit time of 59 ms

0.8 ms for P_{o2}, 41.6±0.9 ms for P_{o3}, and 59.0±0.7 ms for P_{o4} (Fig. 3c). The implicit times of P_{o1} and P_{o2} were slightly longer than P_{i1} and P_{i2}, but that of P_{o3} was not significantly different from that of P_{i3}.

The mean amplitude of the EEPs elicited by 500 μA inward current was 190±26 μV, while that for 500 μA outward current was 150±22 μV (n=6). Because the inward current elicited significantly larger EEPs, we selected the inward current for determining the thresholds.

The EEPs elicited by stimulating with each of the eight electrodes are compared in Fig. 4. Although the overall shape was similar for each of the electrodes, the peak amplitude of the second positive component (P_2) was different. The largest amplitude was elicited by stimulating with electrode c, and it was used for determining the threshold currents.

The EEPs elicited with decreasing inward currents are shown in Fig. 5. For the second (P_2) and third (P_3) peaks, the minimum stimulation current to elicit these peaks was obtained with 50 μA. For the negative components, the first negative peak (N_1) and the second negative peak (N_2) were obtained until 100 μA. The mean threshold current that elicited a small EEP was 55.0±10.0 μA for the six rabbits (27.5±5.0 nC).

The relationship between the averaged peak-to-peak amplitude (P_2 to N_2) of the EEPs and the inward current was

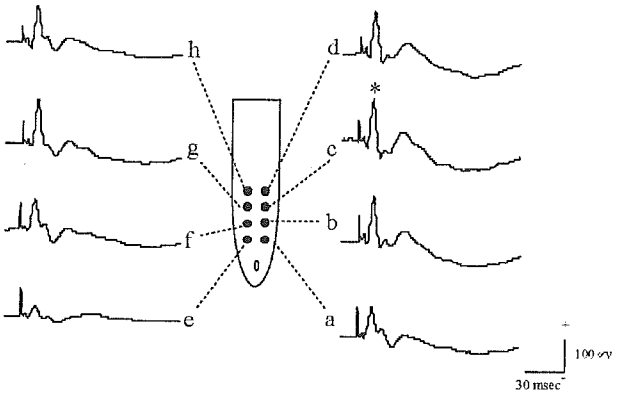

Fig. 4 EEPs elicited by inward electrical pulses from each of the eight electrodes. The amplitude of second positive peak (P_2) varies with the different electrodes. Because electrode c elicited the largest amplitude (*), electrode c was used for determining the threshold electrical current

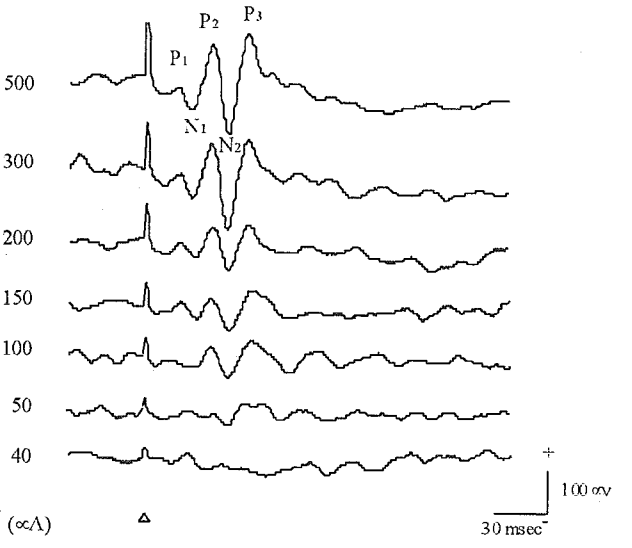

Fig. 5 Changes of the EEP waveforms with decreasing inward electrical currents for stimulation. The second and third positive peaks (P_2, P_3) were detectable with stimulus intensity ≤50 μA. The negative peaks (N_1, N_2) were detectable with stimulus intensity ≤100 μA

examined in the six rabbits (Fig. 6). The regression curve showed that the EEP amplitude increased almost linearly with the lower stimulus currents and tended to be saturated with higher stimulus currents.

Histology

Examination of the histological sections surrounding the implanted electrode showed no obvious damage to the retina, choroid, and sclera at the light-microscopic level. Although a fissure was observed in the sclera which cor-

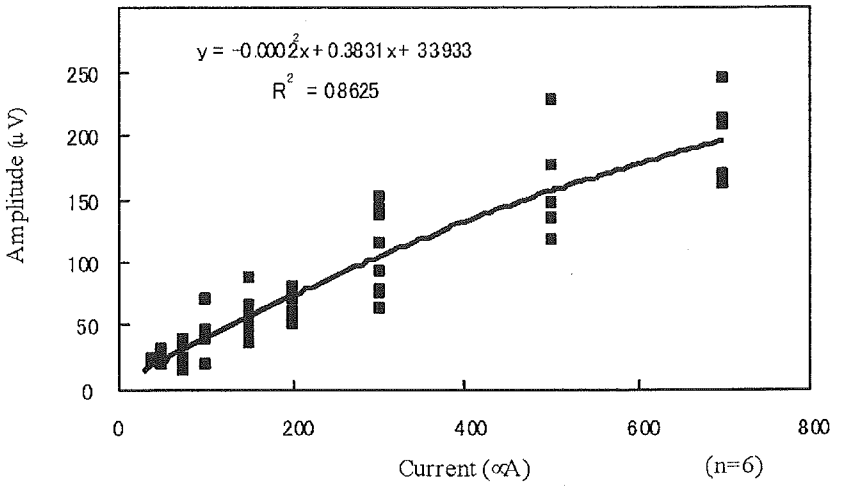

Fig. 6 Averaged peak-to-peak (from P_2 to N_2) amplitude (ordinate) of retinal response elicited by increasing inward current stimulation (*abscissa*). The regression curve shows a slow increase of EEP amplitude with stimulus current amplitude. The increase in the response amplitude is approximately linear with low stimulus current and tended to be saturated with greater stimulus currents

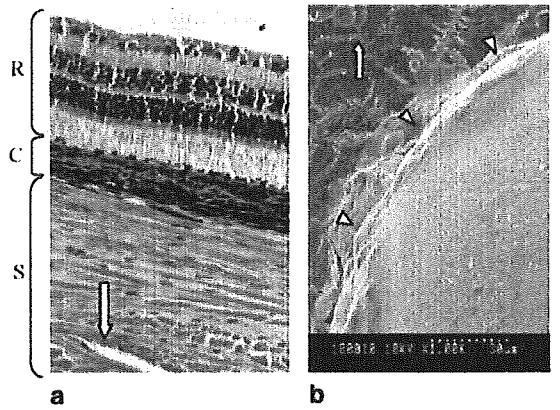

Fig. 7 **a** Histology of the retina and sclera around the electrode. The retina shows no significant damage around the area attached to the array. Degeneration and vacuolization cannot be seen in the sclera and retina. The *arrow* shows the edge of the scleral pocket. *R* Retina, *C* choroids, *S* sclera. HE staining, ×200. **b** A photograph of electrode array surface by scanning electron microscopy. The *arrowheads* point to the electrode surface. There is no deterioration such as cracks on the electrode, only dried crystals (*arrow*) of tissue fluids beside the electrode

responded with the scleral pocket, no significant tissue damage was observed in the sclera (Fig. 7a).

Scanning electron microscopic examination of the electrode also showed no evidence of electrode deterioration such as cracks on the electrode surface but only dried crystals of tissue fluids beside the electrode (Fig. 7b).

Discussion

In this study, we implanted a multichannel electrode array into the sclera. The implantation of electrodes intrasclerally was not difficult, and neither retinal hemorrhage nor retinal detachment was observed during or after the surgery, which suggests the safety of the surgical procedures.

The rabbit retina could be stimulated by STS using electrical currents from multichannel electrodes. The threshold charge for eliciting EEP was 27.5 nC, which is equivalent to a charge density of 56.0 μC/cm^2. Humayun et al. reported that a charge density of 8.92–11.9 μC/cm^2 was required to elicit EEPs from rabbits with epiretinal electrodes [6]. In experiments on cats, Dawson and Radtke found a threshold charge density of 30.5 μC/cm^2 [4]. Chow and Chow implanted their electrodes subretinally in rabbits and reported a threshold charge density of 2.8 nC/cm^2 to elicit EEPs [2]. Although the distance from the electrodes to the retina was farther for our transscleral electrodes than for epi- or subretinal electrodes, the threshold charge density to elicit EEPs was comparable with the other electrode placements.

After changing the polarity to outward currents, the mean threshold was elevated to 75.0 μA (37.5 nC), which was higher than that for inward currents. This finding is consistent with our previous reports that the threshold of inward currents was lower than that of outward currents to elicit EEPs in rats [9].

McCreery et al. reported that the electric charge which can elicit EEPs without damaging the neural tissue was 50 nC or an electrical charge density of 10 μC/cm^2 [12]. This is thought to be the borderline for chronic clinical stimulation; thus, it was recommended that the stimulating electrical current be kept below this charge density. For our system, the electrical charge current was at the upper limit of this borderline, but the charge density exceeded the borderline. Our stimulation method was not a direct stimulation of neural tissue, but an indirect transretinal stimulation. Therefore, the limit of electrical charge density may be expected to be higher than that with direct retinal stimulation.

The retinal origin of EEPs evoked by STS is still unknown. Our previous report [9] showed that STS elicited EEPs without photoreceptors in RCS rat, suggesting that

STS can stimulate the inner retinal neurons. In this study, paying attention to the implicit time of the first EEP peak (P_1) was shorter than that of the first VEP peak (P_{V1}), which suggested that the neuronal processes underlying EEPs by our method were faster than those involved in light stimulation. This shorter implicit time suggests again that STS had elicited EEP by stimulating the inner layers of normal rabbit retina.

The EEP waveforms elicited by intrascleral stimulation were similar to the EEPs elicited by subretinal stimulation [2, 14] or by epiretinal stimulation [13, 16]. They all had several fast wavelets followed by a large slow wave with a latency around 100 ms. Thus, we conclude that we can stimulate the same neural components by intrascleral transretinal stimulation as by epi- or subretinal stimulation.

Our histopathological examinations showed that no obvious damage occurred at the light-microscopic level in the retinal and scleral tissues with the electrical currents used in these acute experiments. Scanning electron microscopy showed no deterioration such as cracks on the used electrode surface. These results showed that the threshold of electric current was low enough to preserve the retinal tissue, and that our stimulating method was also safe.

Although some researchers have reported that the epiretinal [15] and subretinal [3] methods are safe for the retinal tissue, subretinal implantation can cause damage to the outer segments of photoreceptors [14] and induce glial proliferation when chronically implanted [17]. Epiretinal implantation can cause damage around the area of the retinal plug [10, 15], or may be unstable without the use of special devices to fix the electrodes [18]. Our method, on the other hand, requires only scleral surgery and there is no direct invasion of retinal tissue. This simplicity makes the intrascleral electrode insertion a safe and promising method.

In conclusion, our novel surgical procedure, an intrascleral implantation method for STS, represents a safe method for implanting an electrode array in rabbit eyes. EEPs were elicited from the visual cortex with a low electrical current, and the tissue damage was minimal around the electrode. In the future, this method has a potential of increasing the number of electrodes. However, additional studies are necessary to determine the spatial resolution and the long-term effects on the surrounding tissues.

Acknowledgements This study was supported by Health Science Grant, Japan, and by a grant (No. 14571670) from the Ministry of Education, Culture, Sports, Science and Technology, Japan.

References

1. Choudhury DP (1978) Visual field representation in the newborn rabbit's cortex. Brain Res 153:27–37
2. Chow AY, Chow VY (1997) Subretinal electrical stimulation of the rabbit retina. Neurosci Lett 225:13–16
3. Chow AY, Pardue MT, Perlman JI, Ball SL, Chow VY, Helting JR, Peyman GA, Liang C, Stubbs EB Jr, Peachey NS (2002) Subretinal implantation of semiconductor-based photodiodes: durability of novel implant designs. J Rehabil Res Dev 39:313–322
4. Dawson WW, Radtke ND (1977) The electrical stimulation of the retina by indwelling electrodes. Invest Ophthalmol Vis Sci 16:249–252
5. Eckmiller R (1997) Learning retina implants with epiretinal contacts. Ophthalmic Res 29:281–289
6. Humayun MS, Probst R, de Juan E Jr, McCormick K, Hickingbotham D (1994) Bipolar surface electrical stimulation of the vertebrate retina. Arch Ophthalmol 114:40–46
7. Humayun MS (2001) Intraocular retinal prosthesis. Trans Am Ophthalmol Soc 99:271–300
8. Inoue J, Potts AM (1971) Electrically evoked response of the visual system (EER) in the rabbit. Nippon Ganka Gakkai Zasshi 20(75):765–772
9. Kanda H, Morimoto T, Fujikado T, Tano Y, Fukuda Y, Sawai H (2004) Electrophysiological studies on the feasibility of suprachoroidal–transretinal stimulation for artificial vision in normal and RCS rats. Invest Ophthalmol Vis Sci 45:560–566
10. Majji AB, Humayun MS, Weiland JD, Suzuki S, D'anna SA, de Juan E Jr (1999) Long-term histological and electrophysiological results of an inactive epiretinal electrode array implantation in dogs. Invest Ophthalmol Vis Sci 40:2073–2081
11. Margalit E, Maia M, Weiland JD, Greenberg RJ, Fujii GY, Torres G, Piyathaisere DV, O'Hearn TM, Liu W, Lazzi G, Dagnelie G, Scribner DA, de Juan E Jr, Humayun MS (2002) Retinal prosthesis for the blind. Surv Ophthalmol 47:335–356
12. McCreery DB, Agnew WF, Yuen TG, Bullara L (1990) Charge density and charge per phase as cofactors in neural injury induced by electrical stimulation. IEEE Trans Biomed Eng 37:996–1001
13. Nadig MN (1999) Development of a silicon retinal implant: cortical evoked potentials following focal stimulation of the rabbit retina with light and electricity. Clin Neurophysiol 110:1545–1553
14. Schwahn HN, Gekeler F, Kohler K, Kobuch K, Sachs HG, Schulmeyer F, Jakob W, Gabel VP, Zrenner E (2001) Studies on the feasibility of a subretinal visual prosthesis: data from Yucatan micropig and rabbit. Graefes Arch Clin Exp Ophthalmol 239:961–967
15. Walter P, Szurman P, Viobig M, Berk H, Ludtke-Handjery H-C, Deng HR, Mittermayer C, Heimann K, Sellhaus B (1999) Successful long term implantation of electrically inactive epiretinal microelectrode arrays in rabbits. Retina 19:546–552
16. Walter P, Heimann K (2000) Evoked cortical potential after electrical stimulation of the inner retina in rabbits. Graefes Arch Clin Exp Ophthalmol 238:315–318
17. Zrenner E, Stett A, Weiss S, Aramant RB, Guenther E, Kohler K, Miliczek KD, Seiler MJ, Haemmerle H (1999) Can subretinal microphotodiodes successfully replace degenerated photoreceptors? Vision Res 39:2555–2567
18. Zrenner E (2002) Will retinal implants restore vision? Science 295:1022–1025

Transcorneal Electrical Stimulation Rescues Axotomized Retinal Ganglion Cells by Activating Endogenous Retinal IGF-1 System

Takeshi Morimoto,[1,2,3] *Tomomitsu Miyoshi,*[1] *Satoshi Matsuda,*[3] *Yasuo Tano,*[3] *Takashi Fujikado,*[2,3] *and Yutaka Fukuda*[1]

Purpose. To investigate the effect of transcorneal electrical stimulation (TES) on the survival of axotomized RGCs and the mechanism underlying the TES-induced neuroprotection in vivo.

Methods. Adult male Wistar rats received TES after optic nerve (ON) transection. Seven days after the ON transection, the density of the surviving RGCs was determined, to evaluate the neuroprotective effect of TES. The levels of the mRNA and protein of insulin-like growth factor (IGF)-1 in the retina after TES were determined by RT-PCR and Northern and Western blot analyses. The localization of IGF-1 protein in the retina was examined by immunohistochemistry.

Results. TES after ON transection increased the survival of axotomized RGCs in vivo, and the degree of rescue depended on the strength of the electric charge. RT-PCR and Northern and Western blot analyses revealed a gradual upregulation of intrinsic IGF-1 in the retina after TES. Immunohistochemical analysis showed that IGF-1 immunoreactivity was localized initially in the endfeet of Müller cells and then diffused into the inner retina.

Conclusions. TES can rescue the axotomized RGCs by increasing the level of IGF-1 production by Müller cells. These findings provide a new therapeutic approach to prevent or delay the degeneration of retinal neurons without the administration of exogenous neurotrophic factors. (*Invest Ophthalmol Vis Sci.* 2005;46:2147-2155) DOI:10.1167/iovs.04-1339

Injury to retinal ganglion cells (RGCs) causes functional loss of vision that is irreversible because of the limited axonal regeneration of RGCs.[1] Although much research has been performed on the effect of injuries to neurons of the central nervous system (CNS) and on potential therapeutic strategies to promote axonal regeneration, a complete functional recovery has not been achieved and remains a major goal of this area of research.[2]

Axotomy of RGCs has been widely used as an experimental method to investigate whether different agents can protect the RGCs from apoptosis. In rats, axotomy of the RGCs by optic nerve (ON) transection induces apoptosis and results in rapid loss (within 2 weeks) of 85% of the RGC population.[3,4] To protect RGCs from this death, many attempts have been made to administer drugs or genes expressing various neurotrophic factors.[5-11] These trials, however, have had limited success, and many obstacles and negative side effects have arisen that have prevent widespread clinical application of these methods. Thus, it is necessary to devise other treatments using new therapeutic strategies to find a better method to protect damaged RGCs.

Recently, we discovered that direct electrical stimulation of the transected ON increases the survival of axotomized RGCs in vivo.[12] The protective effect of ON electrical stimulation (ONES) suggests that electrical stimulation of neural tissues may be a strategic approach to treat injured axons in the visual pathway. ONES is, however, too invasive to be clinically applicable, and so we tried transcorneal electrical stimulation (TES), which is known to activate inner retinal neurons and to evoke light sensations or phosphenes, in human[13] and animal[14,15] eyes. Its neuroprotective effect, however, has not been examined.

The purpose of this study was to evaluate the effect of TES on the survival of axotomized RGCs in vivo and to determine the mechanism of how TES protects axotomized RGCs. Because it has been reported that the expression of neurotrophic factors can be altered by electrical or physiological stimuli in vivo,[16-19] we hypothesized that TES upregulates some neurotrophic factors and/or their receptors in the retina. The results show that the level of insulin-like growth factor (IGF)-1 increased in the retina after TES and identified Müller cells as the source of IGF-1.

Materials and Methods

Experimental Animals

Adult male Wistar rats (230-270 g) were obtained from SLC Japan, Inc. (Shizuoka, Japan). All experimental procedures were performed in accordance with the ARVO Statement for the Use of Animals in Ophthalmic and Vision Research and were approved by the Animal Research Committee, Osaka University Medical School. The animals were anesthetized with intraperitoneal pentobarbital (50 mg/kg body weight) for all surgical procedures.

Retrograde Labeling of RGCs

To identify RGCs from other retinal cells, they were retrogradely labeled with a fluorescent tracer (Fluorogold [FG]; Fluorochrome Inc., Englewood, CO). A small sponge soaked in 2% FG (in 0.9% NaCl containing 10% dimethyl sulfoxide) was placed on the surface of both superior colliculi after opening the skull dorsal to the lambda fissure.[3,7,12]

From the Departments of [1]Physiology and Biosignaling, [2]Visual Science, and [3]Ophthalmology, Osaka University Medical School, Osaka, Japan.

Supported by Grants-in-Aid for Scientific Research (TMo, TMi, YT, TF); Health Sciences Research Grant from the Ministry of Health, Labour and Welfare, Japan (YT, YF, TF); and the Marine and Fire Insurance Association of Japan (TMi); TMo is a recipient of Research Fellowship of the Japan Society for the Promotion of Science for Young Scientists.

Submitted for publication November 17, 2004; revised January 31, 2005; accepted February 14, 2005.

Disclosure: **T. Morimoto**, None; **T. Miyoshi**, None; **S. Matsuda**, None; **Y. Tano**, None; **T. Fujikado**, None; **Y. Fukuda**, None

The publication costs of this article were defrayed in part by page charge payment. This article must therefore be marked "*advertisement*" in accordance with 18 U.S.C. §1734 solely to indicate this fact.

Corresponding author: Tomomitsu Miyoshi, Department of Physiology and Biosignaling, Osaka University Medical School, 2-2 Yamadaoka, Suita City, Osaka 565-0871, Japan; tmiyoshi@phys2.med.osaka-u.ac.jp.

ON Transection

Seven days after retrograde labeling, the left ON was transected as described in detail elsewhere.[3,4,12] Briefly, a skin incision was made through the left eyelid close to the superior orbital rim, and the orbit was opened. After the superior extraocular muscles were spread, the ON was exposed by a longitudinal incision of the orbital retractor muscle and perineurium. The ON was transected approximately 3 mm from the posterior pole of the eye, with care taken not to damage the retinal blood circulation.

Transcorneal Electrical Stimulation

For electrical stimulation, a noninvasive bipolar contact lens electrode with an inner and outer ring that served as the stimulating electrodes (Kyoto Contact, Kyoto, Japan) was used. Under corneal surface anesthesia by 0.4% oxybuprocaine HCl in addition to systemic anesthesia, the contact lens electrode was placed on the cornea of the eye in which the ON had been transected. Hydroxyethylcellulose gel (1.3%) was applied for corneal protection and for tight adhesion of the electrode to the cornea.

The electrical stimuli consisted of 20 Hz, biphasic rectangular current pulses (100 μA) that were delivered from an isolated constant-current stimulator (Stimulator, SEN-7203; Nihon Kohden, Tokyo, Japan; Isolator, A395R; World Precision Instruments, Sarasota, FL). The electrical stimulation lasted for 1 hour. To evaluate the neuroprotective effect of TES, the pulse duration of electric current was varied from 0 (sham stimulation) to 3 ms/phase. TES was commenced immediately after ON transection.

Quantification of RGC Density

Seven days after ON transection, rats received an overdose of pentobarbital and were perfused transcardially with saline followed by 4% paraformaldehyde (PFA) in 0.1 M phosphate buffer (PB). Both eyes were enucleated, and the retinas were isolated and flatmounted on glass slides. The retinas were examined under a fluorescence microscope (Axioskop; Carl Zeiss, Oberkochen, Germany) with a UV filter (365 nm). The number of FG-labeled neurons was counted in 12 areas (0.5 mm^2 each) at distances of 1, 2, and 3 mm from the optic disc along the nasotemporal and dorsoventral midlines (upper, lower, nasal, and temporal direction). The density of surviving RGCs was calculated from the number of FG-labeled neurons counted in the 12 areas. The data are reported as the mean ± standard deviation.

The statistical significance of differences was determined by one-way ANOVA followed by the Tukey test. Statistical significance was set at $P < 0.05$.

RNA Extraction, RT-PCR, and Northern Blot Analysis

Eyes without ON transection underwent TES for 1 hour, and were removed at different selected time points from 1 hour to 10 days. The retinas were dissected from the eyes in a shallow bath of cold phosphate buffered saline (PBS) and were stored at −80°C until use. Total RNA was then extracted (RNeasy Mini Kit; Qiagen, Hilden, Germany) from pooled retinas and quantified (Gene Quant II; Amersham Pharmacia Biotech, Piscataway, NJ), as previously described.[20]

RT-PCR and Northern blot analysis were performed as previously described.[21] For RT-PCR, 5 μg of total RNA was reverse transcribed using oligo (dT) reverse transcriptase (Ready-To-Go You-Prime First-Strand Beads; Amersham Biosciences). The cDNAs were amplified for 25 to 30 cycles of 30 seconds at 95°C, 30 seconds at 55°C, and 60 seconds at 72°C. The sequences of the primers used were: IGF-1 forward, 5′-TGGACGCTCTTCAGTTCGTG-3′, reverse, 5′-GTTTCCTG-CACTTCCTCTAC-3′; IGF-1R forward, 5′-CAGCTGCAACCACGAGG-CTG-3′, reverse, 5′-GGTTCACAGAGGCGTACAGC-3′; BDNF forward, 5′-AGAGCTGCTGGATGAGGACC-3′, reverse, 5′-CCAGTGCCTTTTGTC-TATCG-3′; TrkB forward, 5′-CTTGGAGAAGGAGCCTTTGG-3′, reverse, 5′-CAACCCGGTAGTAGTCGGTG-3′; bFGF forward, 5′-CGGCAGCAT-CACTTCGCTTC-3′, reverse, 5′-CAGTATGGCCTTCTGTCCAG-3′; FGFR-1 forward, 5′-ACCTGATCTCGGAGATGGAG-3′, reverse, 5′-TGGTGGGT-GTAGATCCGGTC-3′; CNTF forward, 5′-TGAGGCAGAGCGACTCCA-AG-3′, reverse, 5′-GCTCTCAAGTGCTGAGATTC-3′; CNTFR forward, 5′-TTGGGTCACAACACCACGGC-3′, reverse, 5′-CCAAGGAGCTGGTG-GTGCTG-3′; and β-actin forward, 5′-TGCCCATCTATGAGGGTTA-CG-3′, reverse, 5′-TAGAAGCATTTGCGGTGCGGTGCACG-3′.

For Northern blot analysis, total RNA (10 μg) was isolated from the retina at each time point by electrophoresis on 1.0% agarose-formaldehyde gels and transferred overnight onto polyvinylidene difluoride (PVDF) membranes (Millipore Corp., Bedford, MA). The membrane was prehybridized for 1 hour at 65°C in hybridization buffer (0.9 M NaCl, 90 mM sodium citrate [pH 7.0]) containing 5× Denhardt's solution, SDS (0.5%), and heat-denatured salmon sperm DNA (100 ng/mL). The cDNA probe was radiolabeled with [32P]dCTP (NZ522; PerkinElmer Life and Analytical Sciences, Boston, MA, with the Random Primer DNA Labeling Kit, ver. 2; Takara Bio, Shiga, Japan). After hybridization overnight at 65°C in hybridization buffer containing radiolabeled cDNA probe (5 ng/mL), filters were washed twice with 2× SSC, 0.5% SDS and 0.2× SSC, 0.5% SDS for 60 minutes at 65°C, exposed to x-ray film (Fuji Film, Kanagawa, Japan), and subjected to autoradiography. Autoradiograms were quantified by image analysis (Scion Image; Scion Corp., Frederick, MD). The relative expression levels of IGF-1 mRNA in the retinas after TES were compared with the expression in the control retina, which was normalized to 1.0. Data from three independent experiments are given as the mean ± SD.

Western Blot Analysis

Total retinal proteins were extracted from eyes at each time point after TES and were assessed by Western blot analysis, as previously described.[22,23] Total protein was extracted with lysis buffer (50 mM Tris-HCl [pH 7.4]); 0.5% deoxycholate, 1% Triton X-100, 1% NP-40, 10 mM NaF, 150 mM NaCl, 20 μg/mL aprotinin, 20 μg/mL leupeptin, 20 μg/mL pepstatin, 0.5 mM phenylmethylsulfonyl fluoride [PMSF], 1 mM Na_3VO_4, 1 mM dithiothreitol, and 10% SDS) on ice for 30 minutes and centrifuged at 15,000 rpm for 15 minutes at 4°C. The supernatants were collected, and the protein concentration was determined by the Bradford protein assay with bovine serum albumin as a standard (Bio-Rad, Hercules, CA). Total protein (10 μg) was separated by SDS-PAGE (16% Tris-tricine gel; Invitrogen, Carlsbad, CA) and transferred to a PVDF membrane (Millipore Corp.).

Membranes were preblocked in 5% nonfat milk at room temperature (RT) for 1 hour and then incubated with primary antibodies of mouse anti-human IGF-1 (Upstate Biotechnology, Waltham, MA) at a dilution of 1:1000 in TBS and 0.1% Tween 20 (TBS-T) with 5% nonfat milk at 4°C overnight. Membranes were washed in TBS-T and incubated with HRP-conjugated goat IgG secondary antibody against mouse (Jackson ImmunoResearch, West Grove, PA; 1:1000 dilution in TBS-T with 5% nonfat milk) at RT for 1 hour. Labeled proteins were detected by chemiluminescence (ECL; Amersham, Arlington Heights, IL), and the chemiluminescence signals were captured on film (Kodak scientific imaging film; Eastman Kodak, Rochester, NY). Densitometric analyses were then performed (Scion Image; Scion Corp.). First, the relative expression levels of IGF-1 protein were compared with the expression levels of β-actin in the same retinas. Then the values were compared with that of the control retina which was normalized to 1.0. The mean ± SD of three independent experiments was used for the analyses. Experiments for RT-PCR and Northern and Western blot analyses were performed on specimens collected from three animals at each time point, and the results were repeated three times.

Immunohistochemistry

On days 1, 4, 7, or 14 after TES without ON transection, the rats received an overdose of pentobarbital and were perfused transcardially with saline, followed by 4% PFA in 0.1 M PB and the eyes immediately

enucleated. The anterior segment and the lens were removed, and the remaining eyecup was immersed in the same fixative for 30 minutes at 4°C. The eyecups including the ON were cryoprotected in 10% to 20% sucrose in PBS for 2 days, embedded in OCT compound (Tissue-Tek; Ted Pella, Inc., Redding, CA) by snap freezing in liquid nitrogen, and then sectioned (10 μm). The sections were mounted on slides and incubated with blocking buffer (PBS containing 5% goat serum, 5% BSA, and 0.2% Triton X-100) at RT for 1 hour. After three washes in 0.1 M PBS, the sections were incubated overnight at 4°C with a mouse monoclonal antibody against IGF-1 (1:300 dilution; Upstate Biotechnology) and/or a rabbit polyclonal antibody against glutamine synthetase (1:300; Santa Cruz Biotechnology, Santa Cruz, CA) diluted in PBS containing 0.2% Triton X-100, 5% goat serum, and 5% BSA. The sections were then rinsed three times in 0.1 M PBS and incubated with Cy3- and fluorescein isothiocyanate (FITC)-conjugated goat IgG secondary antibodies (1:200; Jackson ImmunoResearch) at RT for 1 hour, followed by three rinses with 0.1 M PBS. The sections were mounted with antifade mounting medium (Vectashield; Vector Laboratories, Burlingame, CA) and examined with a confocal laser microscope (LSM510; Carl Zeiss Meditec).

Administration of IGF-1R Antagonist

JB-3, a selective antagonist for IGF-1R, is a cyclic D-amino acid peptide analogue of the D domain of IGF-1 (CYAAPSAYLKPC).[24,25] JB-3 was synthesized nonbiologically by Sigma Genosys Japan (Hokkaido, Japan). A subcutaneous injection of JB-3 has been shown to inhibit the activity of retinal IGF-1 action in a retinal neovascularization model.[24]

After ON transection, 200 μL of JB-3 solution was dissolved in 0.1 M PBS and was injected intraperitoneally every day for 1 week. For the control, PBS alone was injected. The dose of JB-3 was obtained from the protocol described by Smith et al.[24] This dosage schedule achieved a systemic dose of JB-3 of 10 μg/kg or 100 μg/kg per day, for 6 days.

Results

TES and the Survival of Axotomized RGCs In Vivo

Seven days after the retrograde labeling of the RGCs with FG, the left ON was transected, and TES was immediately applied for 1 hour. The rats were killed 7 days later, and the effect of the TES on the survival of axotomized RGCs was examined in flatmounts of the retina (Fig. 1). In intact control retinas, FG-labeled RGCs were recognized by the fine spots of fluorescence in the perinuclear cytoplasm and proximal dendrites (Fig. 1A). The mean RGC density in the intact control retinas was 2346 ± 175 cells/mm^2 (mean ± SD; $n = 12$; Fig. 2).

Seven days after ON transection and without TES, the number of FG-labeled RGCs was markedly reduced; they were irregularly shaped, and debris of dead RGCs were present (Fig. 1B). The mean RGC density had decreased to 54% of normal ($n = 8$).

The mean RGC density in the sham electrical stimulation was 53% ($n = 6$) of the control retinas. This reduction was not significantly different from that in the eyes with ON transection and without TES. In contrast, retinas that had received TES had many more surviving RGCs than those without electrical stimulation (Fig. 1C). The increase in the densities of RGCs depended on the pulse duration of electric current. TES of 0.5-ms/phase pulse duration significantly increased the number of RGCs (70% of the normal density; $n = 6$, $P < 0.05$). In addition, TES of 1- and 3-ms/phase pulse duration further increased the density up to 85% and 83%, respectively, of normal ($n = 6$, each; Fig. 2). The shapes of surviving RGCs were similar to those of the RGCs in the intact retinas. During the course of these experiments, cataracts or corneal opacities were not developed under surgical microscope in all rats. Fundus examination was performed at the end of TES, but neither retinal detachment nor vitreous hemorrhage occurred in all rats.

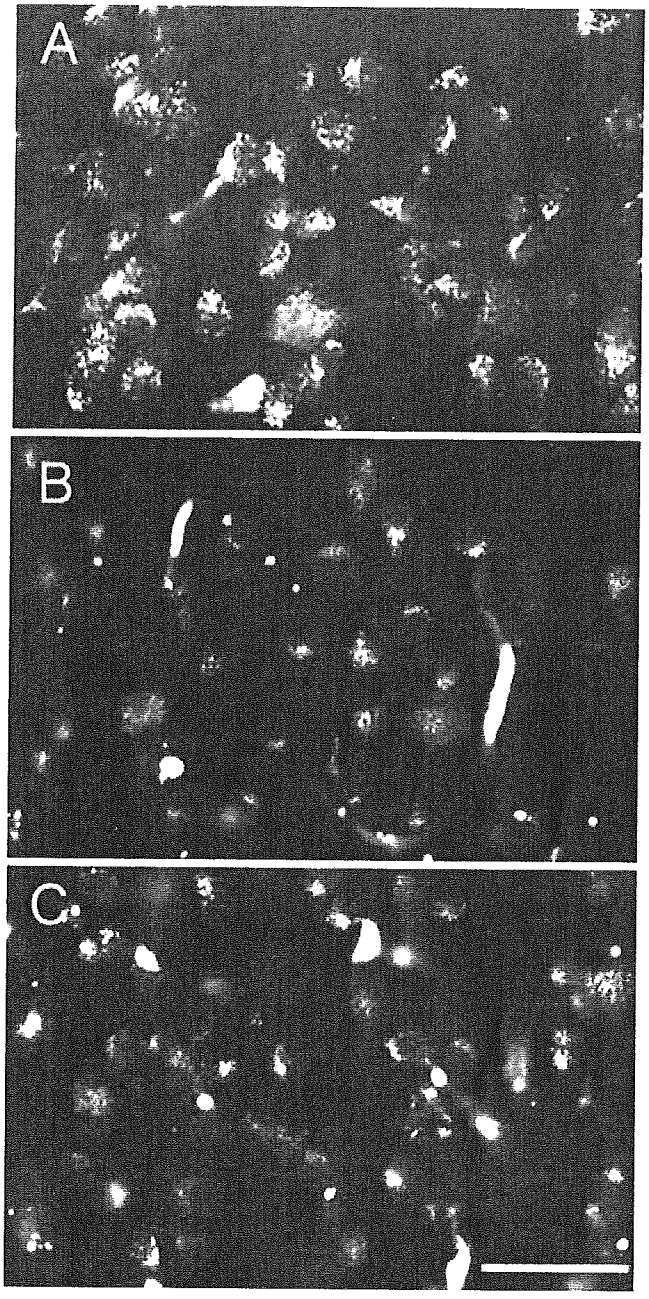

Figure 1. Representative photomicrographs of retrogradely-labeled RGCs in corresponding regions (approximately 1 mm from the optic disc) of flat-mounted retinas. (**A**) FG-labeled RGCs in intact control retina. (**B**) RGCs in the retina 7 days after ON transection without TES. (**C**) RGCs after ON transection with TES (1 ms/phase). More regularly shaped RGCs were seen in the retina after TES than in those without TES. Scale bar, 25 μm.

Increase in Level of IGF-1 after TES

We hypothesized that the neuroprotective effect of TES results from increasing the level of some neurotrophic factors or their receptors in the retina. To test this hypothesis, we examined which genes of the principal neurotrophic factors and their receptors were upregulated after TES (100 μA, 1 ms/phase, 20

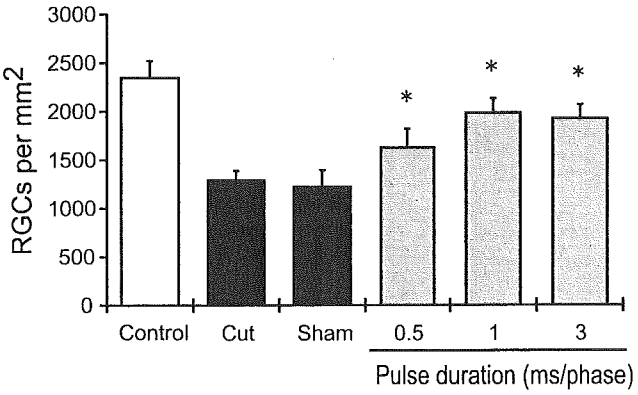

FIGURE 2. The neuroprotective effects of TES on the axotomized RGCs 7 days after ON transection depended on the pulse duration. The density of the FG-labeled RGCs per square millimeter is given as the mean ± SD. Seven days after ON transection, the density of the RGCs decreased to 54% of the control (Cut group). In the sham-treated animals (no electrical stimulation after ON transection), the density decreased to 53% of that of the intact control retina (Sham group). The RGC density in all three groups with TES (0.5, 1, and 3 ms/phase pulse duration) was significantly increased compared with that in the sham group. Statistical analysis was made by one-way ANOVA followed by the Tukey test ($P < 0.01$, $^*P < 0.05$ compared with sham).

Hz, 1 hour) without ON transection. RT-PCR was used to survey the changes in the mRNA expressions of the following neurotrophic factors and receptors: BDNF and its receptor TrkB; CNTF and CNTF receptor-α (CNTFRα); bFGF and FGF receptor-1 (FGFR-1); and IGF-1 and IGF-1 receptor (IGF-1R).

RT-PCR analysis showed that the expression level increased for only the mRNA of IGF-1, and the expression of the mRNA of the other neurotrophic factors and receptors did not change significantly (Fig. 3A). RT-PCR of IGF-1 mRNA also showed that its level of expression depended on the pulse duration of the TES (Fig. 3B). The expression of IGF-1 mRNA in the retina with 1-ms/phase pulses of TES was higher than that with 0.5-ms/phase on day 2 after TES, and this difference was maintained for at least 7 days.

A quantitative analysis of the changes of IGF-1 mRNA expression was also performed by Northern blot analysis at different times, ranging from 1 hour to 10 days after TES. Northern blot analysis showed that the level of mRNA of IGF-1 in the retina gradually increased from day 1 and reached a peak at day 7 (203% of the level of the intact control retina) and remained elevated even at day 10 after TES (Figs. 3C, 3D).

Western blot analysis was also used to determine the level of IGF-1 protein from day 1 to day 14. The level of IGF-1 protein was already increased on day 1 and reached its peak of 189% of the intact control on day 7. The elevated level was still present on day 10, confirming the results obtained from North-

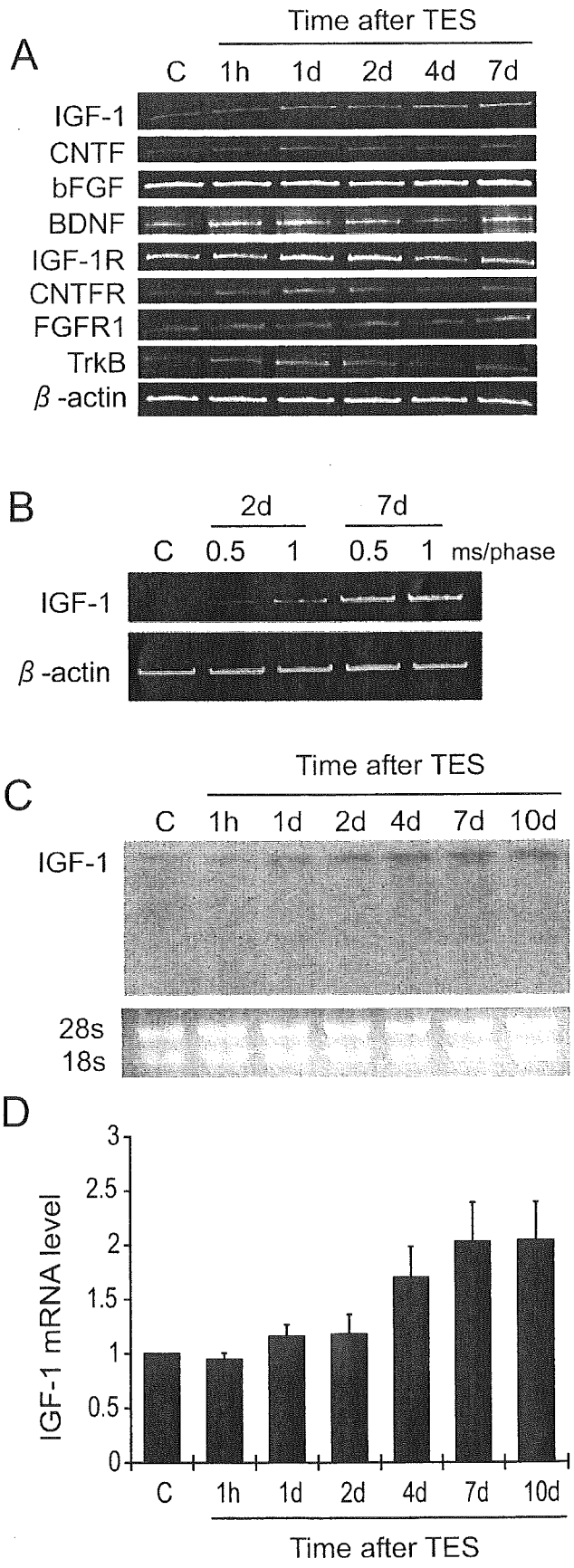

FIGURE 3. Expression of IGF-1 mRNA in the retina after TES. (**A**) RT-PCR analyses for four kinds of neurotrophic factors and receptors at different times ranging from 1 hour to 7 days after TES without ON transection. The data labeled "C" are from intact control retina. (**B**) Electrical current pulse duration-dependent upregulation of IGF-1 mRNA expression by RT-PCR analysis. RT-PCR for β-actin mRNA confirmed that equivalent amounts of RNA were used. (**C**) Northern blot analysis of IGF-1 mRNA in the retina (*top*). RNA loading was measured by gel staining with ethidium bromide (*bottom*). (**D**) Relative expression level of IGF-1 mRNA in retinas after TES compared with the control retinas (normalized to 1.0). The mean ± SD of data from three independent experiments is shown.

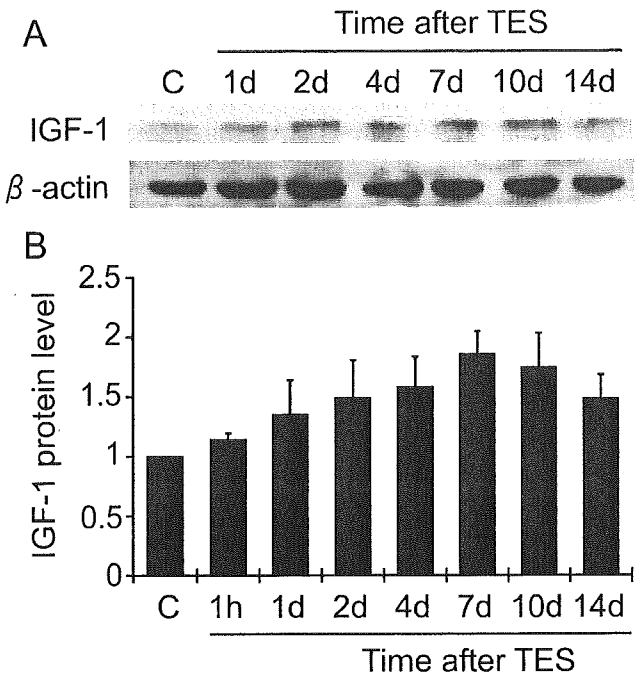

FIGURE 4. Expression of IGF-1 protein. (A) Western blot analysis of IGF-1 protein in the retina (*top*). (B) Relative expression of IGF-1 protein in retinas after TES compared with the contralateral control retinas (normalized to 1.0). Data from three independent experiments were averaged and are presented relative to that in the control retinas (mean ± SD).

ern blot analysis. However, the IGF-1 protein level then decreased on day 14 (Fig. 4).

Immunolocalization of IGF-1 in the Retina after TES

Immunohistochemical studies were performed with IGF-1 antibody, to determine the distribution of IGF-1 protein in the retina from day 1 to day 14 after TES without ON transection. In the intact control retina, IGF-1 immunoreactivity was very weak and restricted primarily to the inner limiting membrane (ILM) and the nerve fiber layer (NFL; Fig. 5A). On day 1 after TES, intense immunoreactivity for IGF-1 appeared from the ILM to the ganglion cell layer (GCL). A weak, but detectable, positive staining was also observed in the inner plexiform layer (IPL) and the inner nuclear layer (INL; Fig. 5B). On day 4, IGF-1 immunoreactivity further expanded, and the radial elements extending from the ILM to the IPL were stained (Fig. 5C). On day 7, the staining for IGF-1 was strongest within the inner retina, and intense staining for IGF-1 was seen in the radial processes of the ILM through the INL (Fig. 5D). On day 14, the immunoreactivity for IGF-1 in the inner retina decreased but IGF-1 signals in the radial processes remained within the NFL and GCL (Fig. 5E).

IGF-1 in Müller Cells

To determine whether Müller cells express IGF-1, additional immunohistochemical studies were performed on the retina with antibodies to IGF-1 and glutamine synthetase (GS), a specific marker for Müller cells. Müller cell bodies lie in a narrow band in the middle of the INL, and their processes span all cellular and plexiform layers of the retina.[26] The coimmunolocalization of IGF-1 (Fig. 5F) and GS (Fig. 5G) was not strong in the Müller cells of the intact retina. This indicates that IGF-1 was located mainly in the basal endfeet of the Müller cells in the intact retina (Fig. 5H). On day 7 after TES, IGF-1 immunoreactivity appeared in the Müller cell processes that extend from the ILM to the OLM and also in the space surrounding them within the IPL and INL (Figs. 5I–K). There was no difference in GS immunoreactivity between the control retina and the retina on day 7 after TES. Examination of the retinas at higher magnification on day 7 after TES showed that strong immunoreactivity of IGF-1 appeared in the endfeet of the Müller cells which surrounded the cells in the GCL (Fig. 5L–N).

We also performed immunohistochemical analysis for glial fibrillary acidic protein (GFAP) which is expressed in Müller cells whenever the retinal neurons are damaged.[27–30] We did not observe immunoreactivity for GFAP throughout the experimental period, suggesting that TES does not damage the retinal tissue (data are not shown). In agreement with the results from Western blot analysis, these results indicated that the IGF-1 is secreted from Müller cells and spreads throughout the inner retina and that TES increases the level of secretion.

Effect of Upregulation of IGF-1 on TES-Induced Neuroprotection of Axotomized RGCs

IGF-1 is one of the trophic factors that promote the survival of axotomized RGCs in vivo.[11] To determine whether IGF-1 is involved in the TES-induced neuroprotection, we counted the number of RGCs that survived after a combined treatment of TES and JB-3, an IGF-1 receptor antagonist.[24,25,31] JB-3 is a long-acting antagonistic peptide that inhibits interaction between IGF-1 and IGF-1R and prevents activation of tyrosine kinase of IGF-1R in a dose-dependent manner.[25,31] Daily injections of low-dose JB-3 (10 μg/kg per day) did not block the neuroprotective effects of TES, since the mean RGC density at day 7 after ON transection was 79% in the intact retina ($n = 4$), which was not significantly different from that after TES and PBS injection (86%; $n = 4$; Figs. 6A, 6B, 7).

However, a high dose of JB-3 (100 μg/kg per day) significantly inhibited the neuroprotective effects of TES, as the number of RGC was reduced to 59% of that in the control retina ($n = 4$; Figs. 6C, 7). With JB-3 alone, the number of surviving RGCs after ON transection (52%; $n = 4$), was similar to that with the ON transection without JB-3 ($n = 8$; Fig. 7). These data showed that the IGF-1 induced by TES plays a key role in TES-induced neuroprotection of axotomized RGCs.

DISCUSSION

Our results demonstrate that TES markedly increased the number of surviving axotomized RGCs in vivo, and the degree of protection was dependent on the strength of the electrical charge. Our results also show that the mRNA and protein of IGF-1 gradually increased in the retina during the 7 days after TES. Immunohistochemical analyses showed that the IGF-1 was located in the endfeet of the Müller cells, and TES led to a spread of IGF-1 in the intact retina. Thus, TES activated the Müller cells to produce more IGF-1 and release it into the inner retina. A blocking of the IGF-1R by JB-3 reduced the degree of neuroprotection by TES on the axotomized RGCs. Thus, TES activates an intrinsic retinal IGF-1 system that then rescues the axotomized RGCs.

IGF-1 as a Key Molecule for TES-Induced Neuroprotection

The upregulation of IGF-1 by the TES proved to be a crucial factor in neuroprotection. To the best of our knowledge, this is the first in vivo demonstration that a neurotrophic factor can be upregulated by electrical stimulation and can then lead to

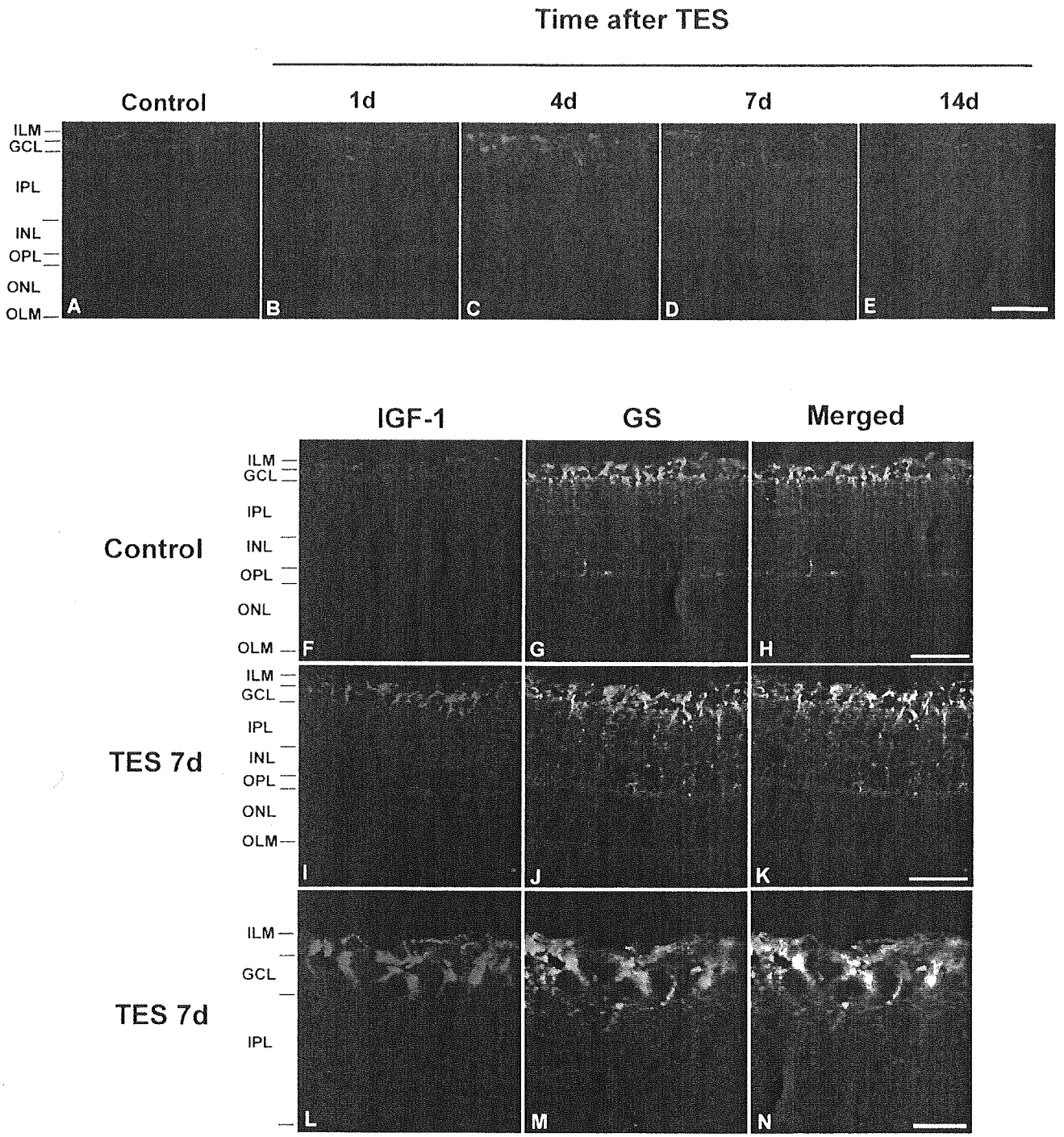

FIGURE 5. Immunohistochemical analysis of IGF-1 in the retina after TES. (**A–E**) Localization of IGF-1 in the retina at different time points after TES. IGF-1 immunoreactivity in the intact retina (**A**). IGF-1 staining increased on day 1 after TES (**B**) and increased more and spread from the ILM to the GCL 4 days after TES (**C**). IGF-1 immunoreactivity reached a peak on day 7 (**D**) and decreased on day 14 (**E**). (**F–N**) Double staining for IGF-1 (*red*) and GS (*green*), a specific marker of Müller cells in the retina. In the intact control retina, weak IGF-1 immunoreactivity was distributed from the ILM to the GCL (**F**), and GS immunoreactivity was present in Müller cells (**G**). The merged image (**H**) shows that weak signal (*yellow*) was localized in the ILM (**H**). Seven days after TES, strong immunoreactivity for IGF-1 appeared from the ILM to the IPL (**I**), and the merged image shows that IGF-1 immunoreactivity appeared in the endfeet and processes of Müller cells (**K**). A high-magnification view of IGF-1 and GS colocalization (**N**) strongly suggests that IGF-1 is produced in the endfeet of Müller cells surrounding the cells in GCL. Scale bars: (**A–E**) 100 μm; (**F–K**) 50 μm; (**L–N**) 20 μm.

neuroprotection. Until now, it has been reported that electrical or natural stimulation can modify the expression of neurotrophic factors or their receptors in neural tissue. Thus, electrical stimulation has been shown to upregulate BDNF and TrkB mRNA in various neurons.[16,17] The mRNA levels of BDNF or TrkB in the rat visual cortex were increased by light stimula-

tion.[18,19] In addition, it has been demonstrated that light-induced damage or mechanical injury to the retina elevates the expression of bFGF and CNTF.[27,28] Because various neurotrophic factors and their receptors are known to exist in the retina,[5,32–35] all of them can be upregulated in the retina by different types of stimuli. However, IGF-1 was specifically upregulated in the retina by TES.

We have shown an upregulation of IGF-1 by Northern and Western blot analyses and immunohistochemistry. We screened for BDNF, CNTF, and bFGF and their receptors in addition to IGF-1 and IGF-1R by RT-PCR, but other neurotrophic factors or receptors may also have contributed to the neuroprotective effects of TES. In addition to the possible upregulation of neurotrophic factors and/or receptors, TES can depolarize the RGCs directly. It has been reported that the neural activity of RGCs increases their sensitivity to peptidic neurotrophic factors.[36,37] We observed that TES of 100 μA at 1 ms/phase, which had been shown to rescue the axotomized RGCs, was also able to evoke electrical responses in the superior colliculus (data not shown). Thus, we cannot rule out the possibility that the electrical activation of the RGCs may have contributed to the effect of IGF-1. However, the systemic administration of JB-3 almost completely inhibited the TES-induced neuroprotection. This clearly shows that IGF-1 is essential for TES-induced neuroprotection, even though some other mechanisms may contribute to the effect of IGF-1.

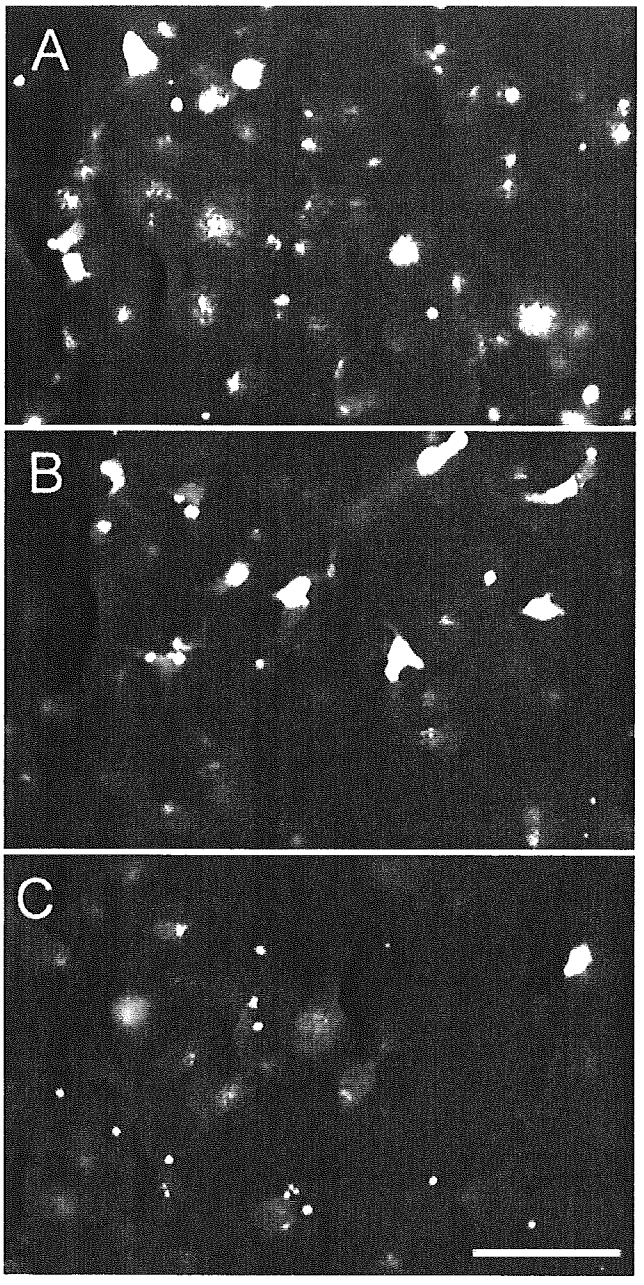

FIGURE 6. Effect of the IGF-1 receptor antagonist JB-3 on neuroprotection by TES. FG-labeled RGCs in the retina 7 days after ON transection. (**A**) Combined treatment with TES and injection of PBS. Combined treatment with TES and daily intraperitoneal injection of (**B**) 10 μg/kg or (**C**) 100 μg/kg JB-3. Scale bar, 25 μm.

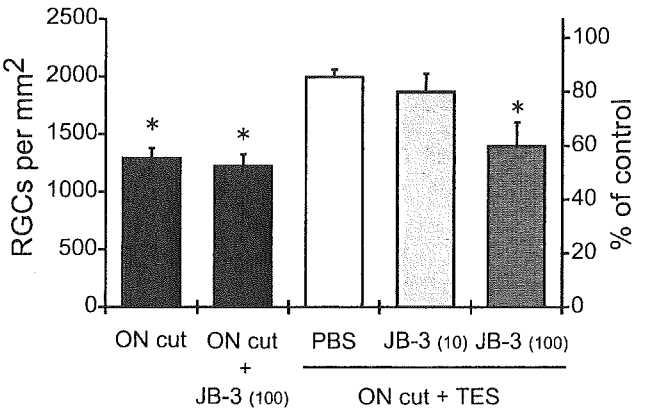

FIGURE 7. Quantitative analysis of the density of surviving RGCs after daily intraperitoneal injections of JB-3 (dose, in micrograms per kilogram per day, shown in parentheses) 7 days after ON transection (n = 4 for each group). Although daily injection of 10 μg/kg JB-3 with TES did not alter the number of surviving RGCs when compared with the treatment combining TES with daily injection of PBS, daily injection of 100 μg/kg JB-3 significantly decreased the number of RGCs. Daily injection of 100 μg/kg without TES, however, did not alter the number of RGCs, compared with ON transection without injection of JB-3 (ON cut). *Statistical significance compared with PBS ($P < 0.05$; one-way ANOVA followed by the Tukey test).

We have demonstrated that electrical stimulation of the stump of the transected ON promoted the survival of axotomized RGCs,[12] and the present study showed that TES, which is less invasive than stimulation of the transected ON, also protects axotomized RGCs from apoptosis. The effect of TES is comparable to that of electrical stimulation to the transected ON.[12] The extent of the neuroprotective effect of TES is also similar to that of intravitreal application of neurotrophic factors.[6,7] The strong effect of TES can be explained by the fact that it upregulated the expression of IGF-1 in the retina for more than 7 days.

Intrinsic Retinal IGF-1 System

IGF-1 has been reported to promote the survival, differentiation, and proliferation of retinal neurons.[38] More specifically, IGF-1 has been reported to promote the survival of injured RGCs, both in vivo[11] and in vitro.[36] In this study, we showed that IGF-1 was recruited from Müller cells by TES and was released to rescue the axotomized RGCs near the Müller cells.

Autocrine-paracrine IGF-1 systems have been reported to exist in the retina.[33,39–42] IGF-1 mRNA was shown to be localized in the GCL in the intact rat retina by in situ hybridization analysis.[33] In contrast, Müller cells express IGF-1 mRNA in vitro.[43] What retinal cells produce and how IGF-1 moves in vivo have not been determined. In the present study, immu-

nohistochemical analyses showed that Müller cells contained small amounts of IGF-1 in their endfeet before TES and that, after TES, Müller cells were activated to increase the level of IGF-1. Our study provides in vivo evidence that the intrinsic IGF-1 paracrine system is in the Müller cells.

The mechanism of the activation of production of IGF-1 by TES has not been determined. It was reported that the regulation of the expression of trophic factors in neurons is clearly linked to their electrical activity. Activation of L-type voltage sensitive Ca^{2+} channels or the non-*N*-methyl-D-aspartate (NMDA) subtype of glutamate receptor leads to an enhancement of BDNF mRNA levels in hippocampal neurons[44,45] and in cortical neurons.[46,47] Similarly, the mechanism for the increased levels of IGF-1 in this study may be related to the electrical activity of retinal neurons and/or glial cells. Further experiments are needed to elucidate this mechanism in detail so that techniques can be designed to stimulate the control glial cells to produce more neurotrophic factors by electrical stimulation.

TES as a New Clinical Technique

Our findings allow us to propose electrical stimulation as a new therapy that activates the intrinsic neuroprotective system. Until now, intravitreal injection or gene transfer of exogenous neurotrophic factors have been used to rescue degenerating retinal neurons[5–11] to provide sustained trophic support. With these methods, however, it is still difficult to deliver exogenous neuroprotective agents chronically into retinal neurons in patients. In addition, intravitreal injection of such neuroprotective agents may cause ocular side effects such as cataract or endophthalmitis. In contrast, TES can control the synthesis of IGF-1, one of the endogenous neurotrophic factors that can then have a neuroprotective effect. This electrical stimulation therapy is simple and less invasive, and ocular side effects were not observed after TES during the course of the study. TES may also have therapeutic or preventive potential in progressive diseases of RGCs, including glaucomatous optic neuropathy. We are now designing a clinical trial using TES for optic neuropathies that are difficult to treat by present methods.

In conclusion, our results showed that TES leads to the upregulation and release of IGF-1 in Müller cells and, consequently, protects the RGCs from secondary cell death after ON transection. Müller cells play an important role in neuroprotection, as well as a housekeeping role that maintains the integrity and the normal function of the retina.

Acknowledgments

The authors thank Yozo Miyake, Hajime Sawai, and Kenji Matsushita for helpful advice and Jun-Sub Choi and Hiroyuki Kanda for technical support.

References

1. Ramon y Cajal S. *Degeneration and Regeneration of the Nervous System.* London: Oxford University Press; 1928.
2. Isenmann S, Kretz A, Cellerino A. Molecular determinants of retinal ganglion cell development, survival, and regeneration. *Prog Retin Eye Res.* 2003;22:483–543.
3. Berkelaar M, Clarke DB, Wang YC, Bray GM, Aguayo AJ. Axotomy results in delayed death and apoptosis of retinal ganglion cells in adult rats. *J Neurosci.* 1994;14:4368–4374.
4. Villegas-Pérez M, Vidal-Sanz M, Raminsky M, Bray G, Aguayo AJ. Rapid and protracted phases of retinal ganglion cell loss follow axotomy in the optic nerve of adult rats. *J Neurobiol.* 1993;24:23–36.
5. Carmignoto G, Maffei L, Candeo P, Canella R, Comelli C. Effect of NGF on the survival of rat retinal ganglion cells following optic nerve section. *J Neurosci.* 1989;9:1263–1272.
6. Mey J, Thanos S. Intravitreal injection of neurotrophic factors support the survival of axotomized retinal ganglion cells in adult rats in vivo. *Brain Res.* 1993;602:304–317.
7. Mansour-Robaey S, Clarke DB, Wang YC, Bray GM, Aguayo AJ. Effects of ocular injury and administration of brain-derived neurotrophic factor on survival and regrowth of axotomized retinal ganglion cells. *Proc Natl Acad Sci USA.* 1994;91:1632–1636.
8. Klöcker N, Braunling F, Isenmann S, Bahr M. In vivo neurotrophic effects of GDNF on axotomized retinal ganglion cells. *Neuroreport.* 1997;8:3439–3442.
9. Clarke DB, Bray GM, Aguayo AJ. Prolonged administration of NT-4/5 fails to rescue most axotomized retinal ganglion cells in adult rats. *Vision Res.* 1998;38:1517–1524.
10. Di polo A, Aigner LJ, Dunn RJ, Bray GM, Aguayo AJ. Prolonged delivery of brain-derived neurotrophic factor by adenovirus-infected Müller cells temporarily rescues injured retinal ganglion cells. *Proc Natl Acad Sci USA.* 1998;95:3978–3983.
11. Kermer P, Klöcker N, Labes M, Bähr M. Insulin-like growth factor-1 protects axotomized rat retinal ganglion cells from secondary death via PI3-K-dependent Akt phosphorylation and inhibition of caspase-3 in vivo. *J Neurosci.* 2000;20:2–8.
12. Morimoto T, Miyoshi T, Fujikado T, Tano Y, Fukuda Y. Electrical stimulation enhances the survival of axotomized retinal ganglion cells *in vivo. Neuroreport.* 2002;13:227–230.
13. Potts AM, Inoue J, Buffum D. The electrically evoked response of the visual system (EER). *Invest Ophthalmol.* 1968;7:269–278.
14. Potts AM, Inoue J. The electrically evoked response of the visual system. 3. Further contribution of the origin of the EER. *Invest Ophthalmol.* 1970;9:814–819.
15. Shimazu K, Miyake Y, Watanabe S. Retinal ganglion cell response properties in the transcorneal electrically evoked response of the visual system. *Vision Res.* 1999;39:2251–2260.
16. Nibuya M, Morinobu S, Duman RS. Regulation of BDNF and trkB mRNA in rat brain by chronic electroconvulsive seizure and antidepressant drug treatments. *J Neurosci.* 1995;15:7539–7547.
17. Al-Majed AA, Brushart TM, Gordon T. Electrical stimulation accelerates and increases expression of BDNF and trkB mRNA in regenerating rat femoral motoneurons. *Eur J Neurosci.* 2000;12:4381–4390.
18. Castren E, Zafra F, Thoenen H, Lindholm D. Light regulates expression of brain-derived neurotrophic factor mRNA in rat visual cortex. *Proc Natl Acad Sci USA.* 1992;89:9444–9448.
19. Bova R, Micheli MR, Qualadrucci P, Zucconi GG. BDNF and trkB mRNAs oscillate in rat brain during the light-dark cycle. *Brain Res Mol Brain Res.* 1998;57:321–324.
20. Nakazawa T, Nakano I, Furuyama T, Morii H, Tamai M, Mori N. The SCG10-related gene family in the developing rat retina: persistent expression of SCLIP and stathmin in mature ganglion cell layer. *Brain Res.* 2000;861:399–407.
21. Yamaguchi A, Taniguchi M, Hori O, et al. Peg3/Pw1 is involved in p53-mediated cell death pathway in brain ischemia/hypoxia. *J Biol Chem.* 2002;277:623–629.
22. Chaum E, Yang H. Transgenic expression of IGF-1 modifies the proliferative potential of human retinal pigment epithelial cells. *Invest Ophthalmol Vis Sci.* 2002;43:3758–3764.
23. Chavez JC, LaManna JC. Activation of hypoxia-inducible factor-1 in the rat cerebral cortex after transient global ischemia: potential role of insulin-like growth factor-1. *J Neurosci.* 2002;22:8922–8931.
24. Smith LE, Shen W, Perruzzi C, et al. Regulation of vascular endothelial growth factor-dependent retinal neovascularization by insulin-like growth factor-1 receptor. *Nat Med.* 1999;5:1390–1395.
25. Pietrzkowski Z, Wernicke D, Porcu P, Jameson BA, Baserga R. Inhibition of cellular proliferation by peptide analogues of insulin-like growth factor-1. *Cancer Res.* 1992;52:6447–6451.
26. Dowling JE. *The Retina: An Approachable Part of the Brain.* Cambridge, MA: Harvard University Press; 1987.

27. Wen R, Song Y, Cheng T, et al. Injury-induced upregulation of bFGF and CNTF mRNAs in the rat retina. *J Neurosci.* 1995;15: 7377–7385.
28. Gao H, Hollyfield JG. Basic fibroblast growth factor: increased gene expression in inherited and light-induced photoreceptor degeneration. *Exp Eye Res.* 1996;62:181–189.
29. Dyer MA, Cepko CL. Control of Müller glial cell proliferation and activation following retinal injury. *Nat Neurosci.* 2000;3:873–880.
30. Chen H, Weber AJ. Expression of glial fibrillary acid protein and glutamine synthetase by Müller cells after optic nerve damage and intravitreal application of brain-derived neurotrophic factor. *Glia.* 2002;38:115–125.
31. Hayry P, Myllarniemi M, Aavik E, et al. Stabile D-peptide analog of insulin-like growth factor-1 inhibits smooth muscle cell proliferation after carotid ballooning injury in the rat. *FASEB J.* 1995;9: 1336–1344.
32. Lin L-F, Doherty D, Lile J, Bektesh S, Collins F. GDNF: a glial cell line-derived neurotrophic factor for midbrain dopaminergic neurons. *Science.* 1993;260:1130–1132.
33. Burren CP, Berka JL, Edmondson SR, Werther GA, Batch JA. Localization of mRNAs for insulin-like growth factor-1 (IGF-1), IGF-1 receptor, and IGF binding proteins in rat eye. *Invest Ophthalmol Vis Sci.* 1996;37:1459–1468.
34. Vecino E, Garcia-Crespo D, Garcia M, Martinez-Millan L, Sharma SC, Carrascal E. Rat retinal ganglion cells co-express brain derived neurotrophic factor (BDNF) and its receptor TrkB. *Vision Res.* 2002;42:151–157.
35. Garcia M, Forster V, Hicks D, Vecino E. In vivo expression of neurotrophins and neurotrophin receptors is conserved in adult porcine retina in vitro. *Invest Ophthalmol Vis Sci.* 2003;44:4532–4541.
36. Meyer-Franke A, Kaplan MR, Pfrieger FW, Barres BA. Characterization of the signaling interactions that promote the survival and growth of developing retinal ganglion cells in culture. *Neuron.* 1995;15:805–819.
37. Shen S, Wiemelt AP, McMorris FA, Barres BA. Retinal ganglion cells lose trophic responsiveness after axotomy. *Neuron.* 1999;23:285–295.
38. Hernández-Sánchez C, López-Carranza A, Alarcón C, de la Rosa EJ, de Pablo F. Autocrine/paracrine role of insulin-related growth factors in neurogenesis: local expression and effects on cell proliferation and differentiation in retina. *Proc Natl Acad Sci USA.* 1995;92:9834–9838.
39. Danias J, Stylianopoulou F. Expression of IGF-I and IGF-II genes in the adult rat eye. *Curr Eye Res.* 1990;9:379–386.
40. Waldbillig RJ, Pfeffer BA, Schoen TJ, et al. Evidence for an insulin-like growth factor autocrine-paracrine system in the retinal photoreceptor-pigment epithelial cell complex. *J Neurochem.* 1991; 57:1522–1533.
41. Moriarty P, Boulton M, Dickson A, McLeod D. Production of IGF-I and IGF binding proteins by retinal cells in vitro. *Br J Ophthalmol.* 1994;78:638–642.
42. Lambooij AC, van Wely KH, Lindenbergh-Kortleve DJ, Kuijpers RW, Kliffen M, Mooy CM. Insulin-like growth factor-1 and its receptor in neovascular age-related macular degeneration. *Invest Ophthalmol Vis Sci.* 2003;44:2192–2198.
43. Li F, Cao W, Steinberg RH, LaVail MM. Basic FGF-induced down-regulation of IGF-I mRNA in cultured rat Müller cells. *Exp Eye Res.* 1999;68:19–27.
44. Zafra F, Hengerer B, Leibrock J, Thoenen H, Lindholm D. Activity dependent regulation of BDNF and NGF mRNAs in the rat hippocampus is mediated by non-NMDA glutamate receptors. *EMBO J.* 1990;9:3545–3550.
45. Zafra F, Castren E, Thoenen H, Lindholm D. Interplay between glutamate and gamma-aminobutyric acid transmitter systems in the physiological regulation of brain-derived neurotrophic factor and nerve growth factor synthesis in hippocampal neurons. *Proc Natl Acad Sci USA.* 1991;88:10037–10041.
46. Ghosh A, Carnahan J, Greenberg ME. Requirement for BDNF in activity-dependent survival of cortical neurons. *Science.* 1994;263: 1618–1623.
47. Tao X, Finkbeiner S, Arnold DB, Shaywitz AJ, Greenberg ME. Ca2+ influx regulates BDNF transcription by a CREB family transcription factor-dependent mechanism. *Neuron.* 1998;20:709–726.

Graefe's Arch Clin Exp Ophthalmol
DOI 10.1007/s00417-006-0260-3

CLINICAL INVESTIGATION

Takeshi Morimoto
Takehiro Fukui
Kenji Matsushita
Yoshitaka Okawa
Hiroshi Shimojyo
Shunji Kusaka
Yasuo Tano
Takashi Fujikado

Evaluation of residual retinal function by pupillary constrictions and phosphenes using transcorneal electrical stimulation in patients with retinal degeneration

Received: 23 July 2005
Revised: 12 December 2005
Accepted: 3 January 2006

This study was supported by Health Science Research Grants from the Ministry of Health, Labor and Welfare, Japan and by a grant from the Ministry of Education, Culture, Science and Technology (no.16591752). T. Morimoto was supported by the JSPS Research Fellowship for Young Scientists.

T. Morimoto · T. Fukui · Y. Okawa · S. Kusaka · T. Fujikado (✉)
Department of Applied Visual Science, Osaka University Graduate School of Medicine,
2-2 Yamadaoka, Suita,
Osaka, 565-0871, Japan
e-mail: fujikado@ophthal.med.osaka-u.ac.jp
Fax: +81-6-68793458

K. Matsushita · H. Shimojyo · Y. Tano
Department of Ophthalmology, Osaka University Graduate School of Medicine,
2-2 Yamadaoka, Suita,
Osaka, 565-0871, Japan

Abstract *Background:* To evaluate inner-retinal function by pupillary constrictions and phosphenes evoked by transcorneal electrical stimulation (TES) in patients with hereditary retinal degeneration. *Methods:* Consecutive 20 eyes of 20 patients (16 with retinitis pigmentosa (RP); and four with cone-rod dystrophy (CRD)) whose visual acuity was equal to or worse than 20/2000 at Osaka University Hospital and eight eyes of eight healthy subjects were enrolled. TES was performed on with a contact lens stimulating electrode. The electrically evoked pupillary response (EEPR) was recorded by a pupillometer, and the phosphenes by the subjective responses. Three electrical current thresholds were determined: T1, threshold current for initial phosphene; T2, threshold for eliciting a phosphene extending into the central field; and P, threshold for a relative pupillary constriction ≥3%. The EEPR and phosphene thresholds were compared with the visual acuity or the visual field. *Results:* All T1, T2 and P were significantly higher in patients than in normals (Mann-Whitney, $P<0.001$). Both T1 and T2 were not correlated with visual acuity but depended on the area and location of the residual visual field. T1 and T2 in RP eyes with a EEPR was significantly lower than that in RP eyes without an EEPR. During TES, all subjects and patients had no pain, and no complications except for a slight corneal superficial punctuate keratopathy. *Conclusions:* The safety and the efficacy of TES to estimate the residual inner-retinal function in patients with retinal degeneration indicate that TES can be used as one of the most important test to select candidates for retinal prostheses.

Keywords Retinitis pigmentosa · Cone-rod dystrophy · Pupillary reflex · Phosphene · Transcorneal electrical stimulation

Introduction

Retinitis pigmentosa (RP) is one of the leading causes of blindness in the world. RP includes a group of heredity retinal degenerations that primarily affects photoreceptor (PR) function [18, 23]. In the last stage of the disease, RP patients have little or no functional vision.

To restore some vision to patients with RP, the strategy of replacing the degenerated photoreceptors by a bionic device called a "retinal prosthesis" is under serious study [17, 36]. Various types of retinal prosthesis have been proposed and tested in animals [2, 8, 11, 13, 16, 28, 34] and patients [3, 10, 26, 33]. A typical retinal prosthesis consists of an array of electrodes that is implanted on the retinal surface and is used to deliver electrical current to the retina to evoke a light sensation called a phosphene.

Another approach to restore vision in RP patient is to transplant retinal progenitor cells (RPCs) into the retina [7, 36]. The success of an artificial retina or the transplantation of RPCs to restore vision depends on the presence of

physiologically intact retinal ganglion cells (RGCs) which can transmit visual signals to the brain.

Morphometric studies of the retinas in RP patients have shown the preservation of some of the RGCs [9, 27, 29]. Postmortem studies of RP eyes have shown that the number of RGC was approximately 30% of that in normal age-matched eyes in the macular area but only 20% in extramacular regions [9, 27]. On the other hand, it must be remembered that remodeling and ectopic retinal structures develop in RP retinas [5, 15]. Retinal remodeling and retinal circuit corruption may prevent the surviving RGCs from transmitting visual signals.

Given these pieces of evidence, a small number of RGCs are certainly present in the eyes of RP patients. However, it is difficult to determine to what extent these RGCs are functional compared with those in an intact retina because the method to evaluate the residual RGC function is limited.

Electroretinography (ERG) and visually evoked potentials (VEPs) are of little value when only a small number of PRs remain in the degenerated retina. On the other hand, electrical stimulation to evoke phosphenes is a potential useful method to evaluate the function of residual RGCs in humans. Phosphenes generated by galvanic or faradaic currents passed through the orbit by various electrode arrangements have been reported since the mid-20th century [1, 6, 19, 20]. More recent studies have used transcorneal electrical stimulation (TES) using corneal electrodes under local anesthesia to evoke phosphenes and to obtain electrically evoked responses (EER) in healthy subjects [21, 24] and RP patients [22, 25].

Although it is not conclusive what kind of retinal neurons are primarily stimulated by TES, the RGCs must be finally activated to transmit visual signals to the brain when a phosphene is evoked. Thus, TES could be one way to estimate the function of the residual RGCs in patients.

The area of the perceived phosphene may correspond to the area where functional RGCs are present and the extent of residual inner retinal function in a degenerated retina. However, it is difficult to assess the RGC function based on the evaluation of phosphene, because phosphene is a subjective sensation. Delbeke et al. tried to compare the phosphenes to somatosensory sensation or pain of the eyelid evoked by electrical stimulation through the eyelid to assess the function of RGCs in patients [4]. Because the somatosensory sensation is also a subjective parameter and is not directly related to phosphenes, the assessment of RGC function based on the somatosensory sensation is limited for candidates of retinal prosthesis [3, 10, 26], even though it is effective for candidates of optic nerve stimulation [33].

Direct and indirect pupillary constrictions can be evoked by TES by stimulating the afferent pupillary pathway and are called electrically evoked pupillary responses (EEPR) [30, 31]. The EEPR can be an objective parameter to be compared with phosphene; however, the relationship between phosphenes and EEPR has not been determined.

Thus, the purpose of this study was to investigate the phosphenes and EEPR in healthy subjects and in patients with retinal degeneration, and to compare these findings to the visual function in these eyes. The long term goal of our studies is to develop a simple and safe method to evaluate the function of the residual RGCs by combining phosphenes and EEPR to select candidates for the retinal prosthesis implant.

Materials and methods

Setting These studies were performed at the Osaka University Medical School, Osaka, Japan.

Patients The characteristics of all subjects are shown in Tables 1 and 2. Eight eyes of eight male volunteers (34±6 years, mean age±SD) with no ocular disorders, and consecutive 20 eyes of 20 patients (51±13 years) with hereditary retinal degeneration [16 patients had RP and four patients had cone-rod dystrophy (CRD)] who visited Osaka University Hospital between January 2003 and December 2003 were studied. The diagnosis was confirmed by independent ophthalmologic and ERG examinations. The inclusion criteria for patients was that the visual acuity was equal or lower than 20/2000, which was lower than the intended resolution of our project of artificial retina. The exclusion criteria were those patients with cardiac pacemaker or the presence of corneal diseases.

All subjects gave an informed consent after the purpose of this study and the procedures to be used were explained. They were free to withdraw at any time. This study adhered to the Declaration of Helsinki and was approved by the Ethics Committee of Osaka University Hospital.

The slit-lamp examination of the corneal was performed just after the TES examination in all subjects.

Table 1 Characteristics of normal subjects

No	Age	Sex	T1 (μA)	T2 (μA)	P (μA)
1	49	M	75	100	125
2	34	M	50	100	125
3	27	M	50	75	125
4	32	M	75	125	150
5	31	M	75	125	150
6	32	M	75	125	150
7	32	M	100	150	200
8	33	M	25	75	75

T1 threshold current of initial perceptual phosphene; *T2* threshold current of phosphene expanding over the center of visual field; *P* threshold current of EEPR

Table 2 Characteristic of patients

No	Age	Sex	VA	T1 (μA)	T2 (μA)	P (μA)	RPC (%)	CVF (deg^2)	PVF (deg^2)	Diagnosis
1	60	F	HM	200	250	600	N	0	1.5×10^3	CRD
2	9	M	20/2000	200	250	250	13	0	1.9×10^4	CRD
3	31	M	20/2000	50	600	600	N	0	7.9×10^3	CRD
4	32	F	20/2000	200	700	300	15	0	1.4×10^4	CRD
5	42	F	20/2000	550	550	N	5.2	1.7×10^2	3.0×10^3	RP
6	51	F	NLP	650	650	NR	NR	0	0	RP
7	50	F	NLP	150	550	NR	NR	0	0	RP
8	23	M	CF	400	400	400	N	0	2.8×10^3	RP
9	45	F	HM	300	350	550	N	3.4×10	0	RP
10	66	F	20/2000	550	700	800	8	4.6×10^2	0	RP
11	44	F	20/2000	600	600	NR	NR	2.9×10	0	RP
12	50	M	20/2000	150	150	600	N	2.5×10	0	RP
13	56	M	HM	550	700	N	2.1	4.1×10	0	RP
14	55	M	HM	1,500	1500	N	4.6	6.1×10	0	RP
15	56	F	20/2000	500	500	1500	7.6	2.0×10^2	0	RP
16	62	F	HM	500	500	900	N	3.4×10	0	RP
17	65	M	LP	1,000	1400	N	N	0	0	RP
18	66	M	LP	1,100	N	N	N	0	0	RP
19	62	F	20/2000	350	700	N	N	2.4×10^2	0	RP
20	66	M	LP	1,400	1400	N	N	0	0	RP

F female, *M* male, *VA* visual acuity; *NLP* no light perception; *HM* hand motion; *CF* counting fingers; *LP* light perception; *T1* threshold current of initial perceptual phosphene; *T2* threshold current of phosphene expanding over the center of visual field; *P* threshold current of EEPR; *RPC* relative pupillary constriction by flash-light stimulation measured by pupillography; *N* not responded; *NR* non-recordable due to nystagmus; *CVF* area of preserved central visual field within a radius of 30°; *PVF* area of peripheral visual field left outside the radius of 30°; *CRD* cone rod dystrophy; *RP* retinitis pigmentosa

Assessment of visual function

The best-corrected visual acuity was measured by a certified orthoptists with a standardized Landolt visual acuity chart. The visual field was quantitatively determined by kinetic perimetry using a Goldmann perimeter. The V/4e target with a luminance of 320 cd/m^2 was projected on a background with a luminance of 10 cd/m^2. The area of the visual fields was calculated using the Scion Image program (Scion Corporation, Frederick, Mass., USA).

Transcorneal electrical stimulation

TES was performed on eight healthy subjects and 20 patients. Before the TES, the cornea was anesthetized with 0.4% oxyburocaine hydrochloride, and the cornea was covered with 3% hyaluronic acid and 4% chondroitin sulfate (Viscoat, Alcon Japan Ltd, Tokyo, Japan) to protect it from injury by the contact lens electrode. A concentric bipolar contact lens electrode (Burian-Allen; Hansen Ophthalmic Laboratories, Iowa City, Iowa, USA) was placed on the cornea, and electric current pulses (20 pulses) were delivered from a stimulator SEN-7203 (Nihonkoden, Tokyo, Japan) and stimulus isolator unit A395 (WPI, Sarasota, Fla., USA) through the two electrodes embedded in the contact lens.

The electrical stimuli were rectangular, biphasic (anodic first) pulses of 10 ms/phase duration, frequency with 20 Hz, and train of 20 paired pulses. These parameters were chosen based on the psychophysical experiment on normal volunteers to elicit phophesene effectively (Matsushita K et al., ARVO abstract 2003). The current intensity ranged from 50 μA to 2 mA with a step of 25 μA up to 100 μA, 50 μA up to 1000 μA, and 100 μA above 1000 μA.

Recording the pupillary constriction

An infrared pupillometer, the IRISCORDER C7364 (Hamamatsu, Hamamatsu, Japan), was used to measure the pupillary responses evoked by TES. The pupillometer is equipped with an infrared charge-coupled device (CCD) camera and recorded the pupillary diameters at a 60 Hz sampling rate. Normal subjects and patients wore a goggle equipped with the CCD camera and the red light-emitting diode (LED) stimulus light (660 nm; maximum light power of 10±3 μW; stimulus duration of 0.1 s). Before inserting the contact lens electrode, the direct and consensual pupillary light reflex of normal subjects and patients were recorded. After inserting the contact lens electrode,

the EEPRs were recorded from the fellow eye. The relative amplitude of the pupillary constriction was determined by calculating the relative amplitude of pupillary constriction starting from the baseline diameter at the stimulus onset to the peak of the pupillary constriction as follows:

$$Relativepupillaryconstruction(RPC\%) = 100(a-b)/a$$

where a=pre-stimulus baseline pupil size (mm), and b=maximally constricted pupil size (mm).

The threshold current for a relative pupillary constriction was determined by the minimal electrical current necessary to elicit an EEPR of ≥3 %.

Psychophysical procedures

We recorded the characteristics of the phosphenes (e.g. location, size, color, brightness, shape) for each electrical current intensity in the dark room. Subjects were masked to the test conditions, as this allowed each subject to provide a non-biased descriptions of their perception. The examiner, who was aware of the stimulus conditions, asked questions about the phosphene. False positive trials (i.e. no stimulus presented) were included to determine the reliability of the responses.

Two thresholds were determined; threshold 1 (T1) was defined as the value of the electrical current that elicited the first perceived phosphene anywhere in the visual field, and threshold 2 (T2) was the value at which the subjects perceived a phosphene extending into the center of the visual field. We determined the two thresholds by starting with a current intensity below threshold and increasing the stimulus strength stepwise until a perception of a phosphene was first perceived (T1a), and the current at which the phosphene extended into the central visual field (T2a). Next, the stimulus strength was started well above threshold and reduced along the same steps until the same perceptions were obtained, i.e. disappearance of the phosphene from the central visual field (T2b), and the complete disappearance of a phosphene (T1b). T1a and T1b are usually the same but if the values differed, we averaged the two values to determine the threshold (T1). The same procedure was taken to determine the value of T2. For each step, the patient was asked to describe his/her perceptions in detail which were recorded on audio tape.

Statistical analyses

Data are presented as the means±standard error of the means (SEM), and statistically analyzed with the SPSS 10.0J program (SPSS Inc, Chicago, Ill., USA). Comparisons between two groups were made by the student *t*-test when data were normally distributed, or by the Mann-Whitney *U*-test when data were not normally distributed. The degree of correlation was evaluated by the coefficient of correlation (r) calculated using Pearson correlation coefficient. Comparisons between the three groups were made by one-way ANOVA followed by the Tukey test when data were normally distributed. The probability level is represented as the value "*P*"; statistical significance was set at $P<0.05$.

Results

Characteristics of phosphenes in normal subjects and patients

In normal subject, phophene was first perceived in the upper or lower peripheral field with the mean threshold of 65±8 μA (T1). With a further increase in the current intensity, phosphene spread into the center of the visual field with the mean threshold of 109±9 μA (T2). With a further increase in the current intensity, a pupillary constriction was evoked with a mean intensity to evoke a RPC of just >3% was 138±13 μA (P). A comparison of the three thresholds, T1, T2, and P, showed that they were significantly different from each other ($P<0.001$, one-way ANOVA) (Table 1, Fig. 1).

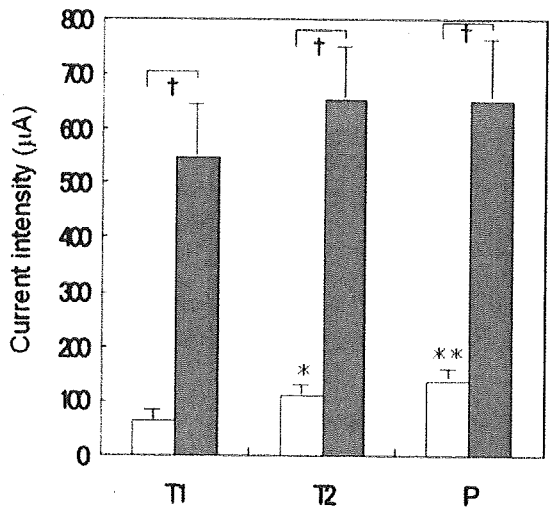

Fig. 1 Average threshold current intensities of phosphenes and pupillary constrictions in normals (*open bar*) and in eyes with retinal degeneration (*filled bar*). *T1* threshold current intensity of initial phosphene, *T2* threshold current intensity for phosphene covering the center of visual field, *P* threshold current intensity of electrically evoked pupillary response (*EEPR*) . Data are presented as mean± SEM. There was a significant difference among three thresholds in normals (one-way ANOVA, $P< 0.01$; Tukey test, * $P<0.05$, ** $P<0.01$, vs T1). No significant difference among three thresholds was obtained in eyes with retinal degeneration. There was a significant difference in each threshold between normals and retinal degeneration (Mann-Whitney Rank Sum Test,† $P<0.001$)

The distribution of the T1, T2, and P thresholds in patients are shown in Table 2. A phosphene was elicited by TES in all patients. However, the threshold currents were much higher than normal subjects and varied considerably among patients. The mean T1 threshold was 545±411 μA. With an increase in the current intensity, many patients reported that bright light sensation spread toward the center of visual field. The mean T2 threshold was 723±479 μA. However patient 18, mentioned that the phosphene did not spread into the center with maximum current intensities (2000 μA). The threshold of P was higher than T2 in most cases but in some patients, pupillary reflex was not evoked with the maximum current intensities (2000 μA) (Table 2, Fig. 1). The false positive rate was 0% in the subjective phosphene test.

Relationship between thresholds (T1 and T2) in patients and normal subjects

Although the thresholds of the normal subjects were quite comparable, the thresholds of the patients varied considerably. A scatter plot of T2 as a function of T1 in normal subjects and patients is shown in Fig. 2. In the normal subjects, a highly significant positive correlation was observed between the T1s and T2s (r=0.900 and P=0.002; Pearson's correlation coefficient).

The patients, on the other hand, were divided into two groups from the scatter plot. One group was made up of patients whose thresholds were distributed tightly around the linear regression line of normal subjects, and the thresholds of other group of patients were shifted above the line. These results lead us to examine whether the thresholds in the patients were dependent on the visual acuity or the residual visual field or the type of disease.

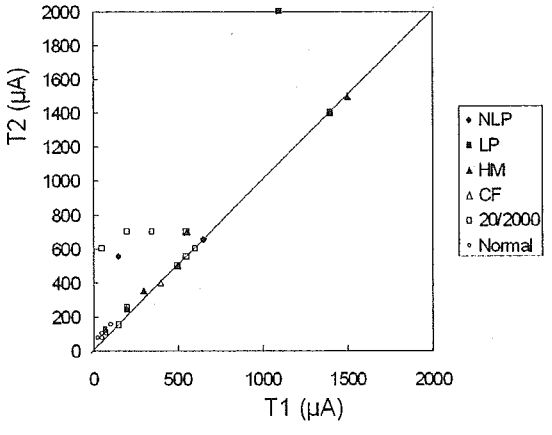

Fig. 2 Comparison of T1 with T2 in normal subjects and patients. Normal subjects (*open circles*) and patients (*filled circles*) are plotted. Patients were divided into two groups. One group includes patients with a closer fit to the linear regression line of normal subjects, another group included patients distributed above the line

Relationship between thresholds and visual acuities in patients

The visual acuities were converted to the logarithm of the minimum angle of resolution (logMAR) units for the statistical analysis. For visual acuities less than 20/2,000 (2.0 logMAR units), the following log MAR values were assigned [12]: 2.6 logMAR for counting finger (CF); 2.9 logMAR for hand motion (HM), 3.1 logMAR for light perception (LP); and 3.4 logMAR for no light perception (NLP). The relationship between the electrical phosphene thresholds and logMAR visual acuities is shown in Fig. 3. There was no significant relationship (T1,r=0.433; P=0.056: T2,r=0.417; P=0.067) between log MAR visual acuities and thresholds (Fig. 3a,b). For example, although patients 6 and 7 were NLP, their thresholds were lower than those of 11 and 14, whose visual acuities were 20/2000 and HM, respectively (Table 2).

Relationship between thresholds of phosphenes and residual visual fields in patients

The patients were classified into three groups on the basis of the location of residual visual field: type C, visual field present within the central 30° radius (n=10); type P, peripheral visual field left beyond the central 30° radius (n=5); and type N, complete loss of visual field (n=5). A patient who had two islands of visual field with one located within 30° radius was categorized as type C.

The relationship between the thresholds and type of residual visual fields is shown in Fig. 4. There was a significant difference in the thresholds for a phosphene in the three groups (one-way ANOVA, T1, T2; P<0.05). The mean current intensities of T1 and T2 for type P patients were the lowest among the three groups: T1=210±56 μA; T2=440±91 μA, and for type C: (T1; 555±114 μA, T2; 625± 112 μA), and the mean intensities in type N were much higher (T1; 860±214 μA, T2; 1200±269 μA) (Fig. 4).

We further analyzed the relationship between the area of residual visual field and thresholds in each groups, and no significant correlation was found.

Relationship between thresholds of phosphenes and type of disease

In eyes with CRD, the cones are predominantly damaged and the loss of cones result in a loss of the central visual field, while in RP, the rods are predominantly damaged and the loss of rods result in a loss of the peripheral visual field. We therefore divided eyes with retinal degeneration into the CRD group and RP group (Fig. 5, Table 2).

The mean current intensity of T1 in the RP patients was significantly higher than that in CRD patients (640± 101 μA vs 163±38 μA, P<0.05; Fig. 5e). Although the

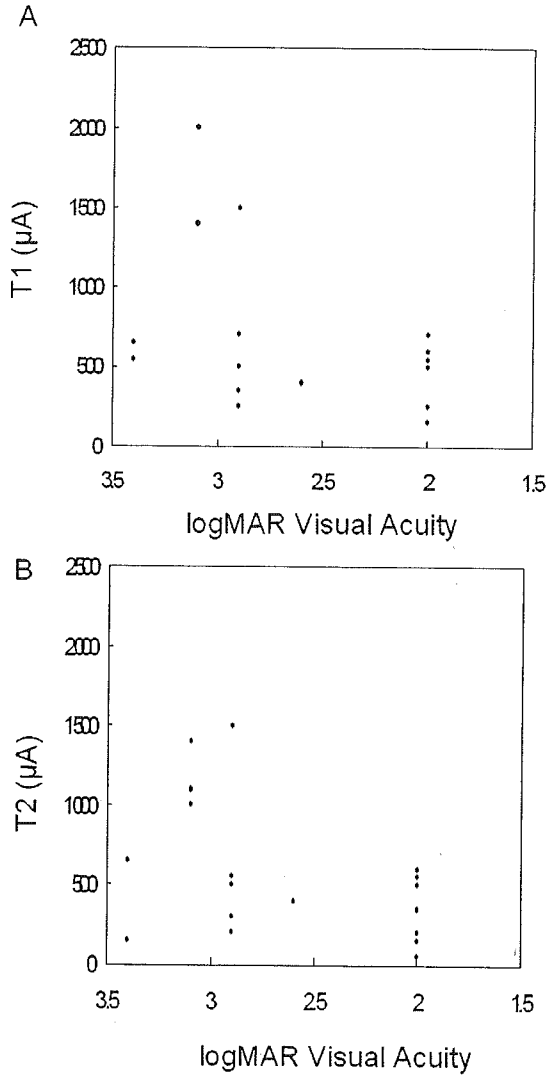

Fig. 3 Relationship between T1 and T2 and logMAR visual acuities in patients. **a**. T1s are plotted versus logMAR visual acuities, **b**. T2s are plotted versus logMAR visual acuities. There was no significant correlation between thresholds and logMAR visual acuities

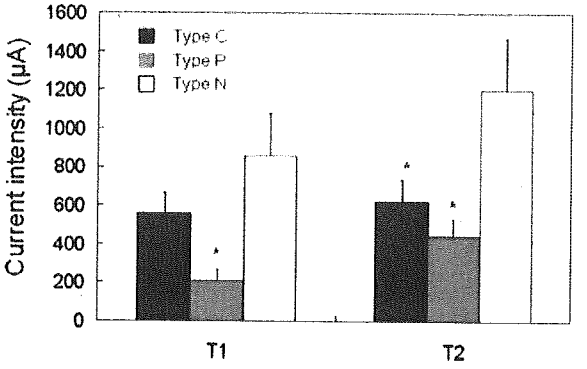

Fig. 4 Comparison of the type of residual visual fields with thresholds of phosphene. Type C; central visual field preserved within a 30° radius; type P, peripheral visual field left outside the central 30°; type N; complete loss of visual field. Data were presented as mean±SEM. There was a significant difference between three thresholds (one-way ANOVA: T1, T2; $P<0.05$; Tukey test, * $P<0.05$ vs type N)

mean current intensity of T2 in the RP patients was higher than in the CRD patients, the difference was not significant (790±126 μA vs 440±91 μA).

Relationship between pupillary responses and thresholds in RP patients

An EEPR was examined in all but three RP patients. These three had nystagmus and the tests for an EEPR could not be performed, and they were excluded from the analysis. An EEPR was recorded from all eyes with CRD, but 54% (7/13) of the RP eyes did not show a positive EEPR (Fig. 6a).

The RP patients were classified into four groups on the basis of the presence or absence of a light and electrically-elicited pupillary response: type I, 15% (2/13) had light reflex (+) and EEPR (+); type II, 31% (4/13) had no light reflex (−) and had an EEPR (+); type III, 23% (3/13) had light reflex (+) and no EEPR (−); and type IV, 31% (4/13) had no light reflex (−) and no EEPR (−).

The waveform of the EEPR was very similar to that of the light response (Fig. 6a).

We examined the relationship between EEPR and thresholds of phosphenes in RP patients. We compared the thresholds of RP eyes that had a EEPR to those who did not have a EEPR. The absence or presence of EEPR completely divided patients into high or low thresholds groups. In the group with an EEPR, the mean current intensity of T1 was 400±62 μA, and the mean intensity of T2 was 433±75 μA. On the other hand, in the group without an EEPR, the mean intensities of T1 and T2 were significantly increased to 921±169 μA and 1,179±203 μA, respectively (T1, $P<0.05$; T2, $P<0.01$; Fig. 6b).

Side effects of TES examination

During the TES examination, no subjects complained pain or irritable sensation on cornea or upper lid. The slit-lamp examination after TES examination revealed a slight superficial punctuate keratopathy in all cases, which was comparable to those observed after the routine examination of electro-retinography.

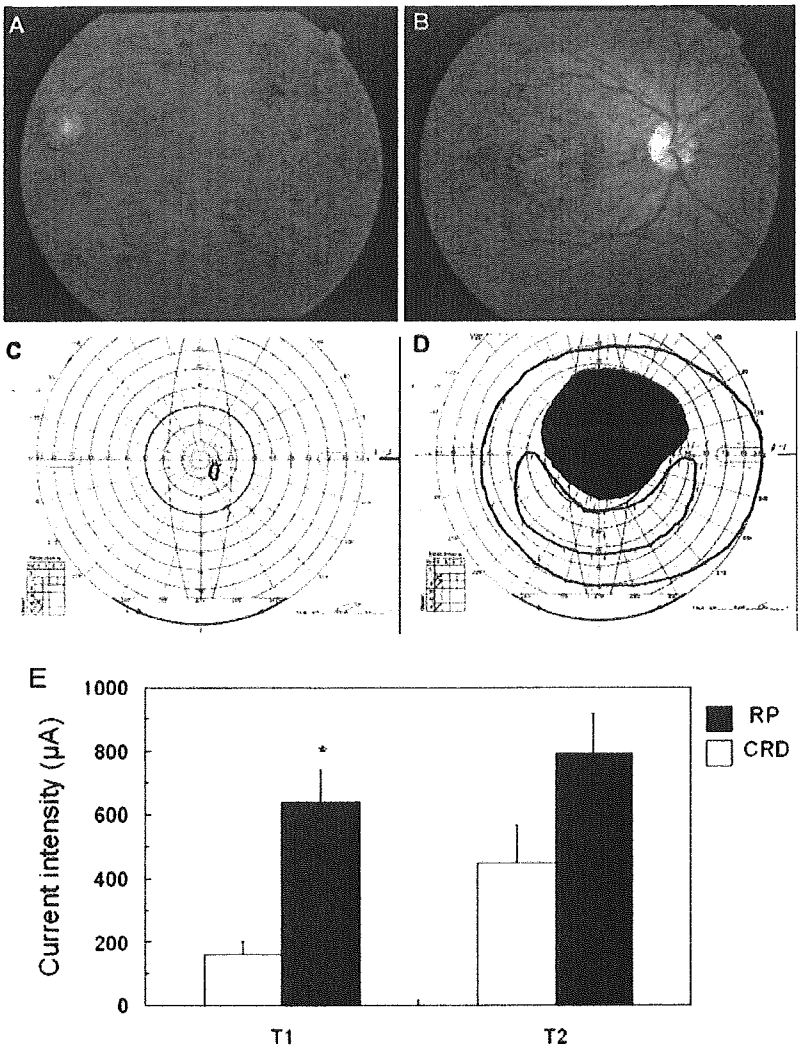

Fig. 5 Comparison of mean thresholds of RP patients with those of CRD patients. Representative fundus photographs and visual fields from two types of patients; **a** and **c** from a RP patient, **b** and **d** from a CRD patients. **e**. Mean thresholds of phosphene in two types of patients. There was a significant difference of T1 between the two groups (*, Mann-Whitney *U*-test, $P<0.05$); however, there was no significant difference in T2 between them

Discussion

Except a slight superficial punctuate keratopathy, no side effect was observed during or after TES, indicating that TES is a safe examination when performed along with our protocol.

The computer simulation showed that the charge density in the peripheral retina was higher than in the central retina if an eye was stimulated by a concentric corneal electrode [14], which was consistent with the observation that T2 was larger than T1. In order to elicit EEPR, more current was needed, suggesting that a more number of RGS should be involved to elicit pupillary reflex than to perceive phophene (Fig. 1).

A possibility that a direct current affected the pupil efferent and elicited the EEPR was neglected by the report that in eyes of optic atrophy, EEPR was not induced in the contra lateral healthy eye [32].

All RP patients perceived a phosphene, but the average threshold current of T1 or T2 was 7–8 times greater in RP patients than in normal subjects, suggesting that the number of residual RGC was much smaller in RP patients than in normal subjects [9, 27]. (Fig. 1). The threshold current of phosphenes varied among the patients, indicated that the residual RGCs function varied among patients (Table 2).

A plot of T1 and T2 in normal subjects and patients showed two groups. In one group, T2 was highly correlated with T1 as in normal subjects, and in the other group, the T2 was elevated relative to T1 (Fig. 2). These results indicate that in the former group, the rate of RGC loss in macula area may be similar to that in the extramacular area as reported [9, 27, 29], while in the latter group, the degree of RGC loss in the macula may be higher than that in the extramacular area.